AFCRL-62-222

CONFINEMENT OF A PARTIALLY IONIZED GAS BY A PERIODIC MAGNETIC FIELD

BY

BERT ZAUDERER

MAGNETOGASDYNAMICS LABORATORY
REPORT NO. 62-2
DEPARTMENT OF MECHANICAL ENGINEERING
MASSACHUSETTS INSTITUTE OF TECHNOLOGY

Contract AF 19(604)-4551
Project 8608
Task 86081

JANUARY 1962

Prepared for
GEOPHYSICS RESEARCH DIRECTORATE
AIR FORCE CAMBRIDGE RESEARCH LABORATORIES
OFFICE OF AEROSPACE RESEARCH
UNITED STATES AIR FORCE
BEDFORD, MASSACHUSETTS

AFCRL-62-222

CONFINEMENT OF A PARTIALLY IONIZED GAS BY A PERIODIC MAGNETIC FIELD

by

Bert Zauderer

Magnetogasdynamics Laboratory
Report No. 62-2
Department of Mechanical Engineering
Massachusetts Institute of Technology

Contract AF 19(604)-4551
Project 8608
Task 86081

January 1962

Prepared for

GEOPHYSICS RESEARCH DIRECTORATE
AIR FORCE CAMBRIDGE RESEARCH LABORATORIES
OFFICE OF AEROSPACE RESEARCH
UNITED STATES AIR FORCE
BEDFORD, MASSACHUSETTS

62-3-1

Requests for additional copies by Agencies of the Department of Defense, their contractors, and other Government agencies should be directed to the:

ARMED SERVICES TECHNICAL INFORMATION AGENCY
ARLINGTON HALL STATION
ARLINGTON 12, VIRGINIA

Department of Defense contractors must be established for ASTIA services or have their 'need-to-know' certified by the cognizant military agency of their project or contract.

All other persons and organizations should apply to the:

U. S. DEPARTMENT OF COMMERCE
OFFICE OF TECHNICAL SERVICES
WASHINGTON 25, D. C.

ABSTRACT

Two sets of experiments were performed to test the possibility of confining a partially ionized gas by a periodic magnetic field, such that the density of un-ionized gas in contact with the wall be small compared to the density of the magnetically confined plasma.

In the first set of experiments, on argon plasma with a 10,000°K temperature, and about 20% degree of ionization was produced in a 6" diameter combustion driven shock tube. When the plasma was inside a coaxial 14" diameter solenoid, a 67 Kc magnetic field was turned on. When the static plasma pressure was less than the magnetic pressure, $B^2/2\mu_o$ a smear camera photograph, showed periodic contractions of the plasma cylinder at a rate equal to twice the field frequency. From the smear photograph and magnetic probe measurements inside the shock tube it was concluded that the outer cm, layer of the plasma was substantially heated and ionized by eddy current heating. When $p/B^2/2\mu_o$ was equal to 0.26, magnetic probes showed that the boundary of the ionized portion of the gas was located between $1\frac{1}{2}$ cm and $2\frac{1}{2}$ cm from the wall. Since the edge of the gas was highly ionized it was concluded that a large percentage of the gas was confined by the field.

In the second set of experiments on electrodeless ring discharge was used to produce an argon plasma in the same experimental arrangement as in the previous

experiments. Smear photographs showed that radial shocks were formed at the inside wall of the glass tube every half field cycle and they propagated toward the axis of the tube with velocities between 0.4 and 1.0 cm/μ. sec. The gas temperature was estimated as being between 10,000°K and 20,000°K. Magnetic probes inside the glass tube indicated that qualitatively the magnetic effects were similar to the first set of experiments and that the field was confining the plasma. A similar ring discharge experiment in Hydrogen led to the conclusion that the speed of sound divided by the tube diameter must be very small compared to the angular field frequency to obtain a steady continuous confinement of the plasma by the field.

I. INTRODUCTION

Butler (1) has discussed the possibility of confining a thermonuclear plasma by a periodic, microwave frequency, magnetic field. The containment criteria are: a) $\delta < D/2$, where δ is the skin depth of the field inside the plasma and D is the plasma diameter; and b) $a/2\pi D << f$, where a is the speed of sound of the plasma, and f is the field frequency. These two criteria could also be applied to a low temperature (approximately 10,000°K) plasma, such as a fissionable plasma in a "cavity" reactor (2). At temperatures of 10,000°K contact of the plasma with the walls is not as critical as at fusion temperatures, where impurity atoms can cause severe radiation cooling. Therefore, in this paper, a plasma will be considered "confined" by a magnetic field, if the density of the plasma in contact with the walls is small compared to the density of the main plasma body confined by the field.

The purpose of the experiments reported in this paper, was to determine whether Butler's containment criteria can be applied to a low temperature plasma. A cylindrical 15 cm diameter, argon plasma, at 10,000°K, in a coaxial 100 Kc field, theoretically satisfies both containment criteria a) and b). The 100 Kc field was obtained by discharging a high frequency capacitor into a solenoid. Two methods were used to obtain the argon plasma. One method, which produces a uniform plasma with known properties employs a 15 cm diameter combustion driven shock tube. The physical principles of the shock tube are discussed by Resler (3).

Another way to produce a plasma is to utilize the induced circumferential electric field in a solenoid, ($E = dB/dt$), to produce a "ring" discharge in argon at a few hundred microns pressure. Very little accurate data exists on the ring discharge breakdown fields (4). Blackman(5) performed a ring discharge experiment using a single turn coil wrapped around a cylindrical discharge tube filled with argon. By discharging a capacitor into the coil at 380 Kc he observed that breakdown occurred at the start of the second half cycle (when $B = 0$ and dB/dt is a maximum). The breakdown field was a function of the gas pressure and had a similar shape to the DC Paschen Curve. The minimum breakdown voltage was 380 Volts/cm and it occurred at 0.3 mm Hg pressure.

In an early experiment on the fusion device called Scylla, Bullis (6) observed in a ring discharge in deuterium, that when the magnetic pressure, $B^2/2\mu_o$, was much greater than the gas pressure, strong radial shocks compress (every half cycle) the gas and heat it to high temperatures. In his experiment, the speed of sound of the shock heated D_2 was so high that $a/2\pi D = f$, and hence he did not obtain continuous AC containment.

Based on the above experimental results one can conclude that a ring discharge can be utilized to study high frequency magnetic containment by a proper choice of experimental variables. In the experiments reported in this paper a high molecular weight gas (Argon) was used to study AC containment under conditions which would satisfy Butler's containment criteria. To study the effect of the speed of sound of the gas, a ring discharge experiment was performed using Hydrogen in the discharge tube, and the same field frequency as in the argon experiments.

II. APPARATUS

Design of Apparatus

1. The shock tube: To produce a uniform argon plasma, a 6" diameter shock tube was chosen, because the initial pressure can be as low as 100 microns (8, 7). However, 100 microns is the lowest initial pressure in which a chemical shock forms, hence increasing the tube diameter above 6" is of no advantage. The advantage of a low initial pressure is that the radiation cooling behind the shock is very small, hence, one obtains a uniform plasma slug. Argon was chosen as the driver gas because it has been extensively studied (3, 9, 10, 11). The $1\frac{1}{2}$" diameter shock tube is described by Resler (3). In this experiment a $1\frac{1}{2}$" to 6" expansion nozzle was placed downstream of the high pressure diaphram and the entire driven section, including a glass test section, had a 6" diameter.

2. The capacitor and field coil: By a suitable choice of the driver to driven pressure ratio, the shock tube can readily produce an argon gas temperature of 10,000°K and a conductivity of 4000 mhos/meter. For these conditions one finds that a field frequency of 100 KC will satisfy both of Butler's containment criteria since δ is equal to 3 cm and $a/2\pi D$ is equal to 2 KC for the argon plasma. Using standard techniques (12) one can calculate that the field coil has one turn with a 14" diameter and 16" length. The capacitor used had a rating of 14 μf., 20 KV. Figure 1 shows the experimental set up of the field coil and shock tube.

Instrumentation

1. Magnetic probes: Magnetic probes were used to measure the strength and distribution of the field inside the solenoid with and without a plasma inside it. In Figure 2 the location of the various probes are shown. Probe No. 4 measured the total flux inside the shock tube while Probe No. 7 measured the local field inside the plasma. Measurements with Coil 7 were made at r/r_o = 0.83, 0.66 and 0.33 where r_o is the I. D. of the shock tube. Probe 1 measured the total current per unit length inside the solenoid and Probe 5 was used to monitor the external field when the plasma was inside the solenoid. This was done by connecting probe 7 and 5 to the two sweeps of a 555 Tektronix Dual beam oscilloscope. Both sweeps had the same time base.

2. The rotating mirror camera: The glass test section of the shock tube was covered with tape and a vertical slit (Figure 1) was uncovered in the central plane of the solenoid. A rotating mirror camera was used to photograph the dynamic effects of the field plasma interaction. Since the rotating mirror was horizontal, three first surface mirrors were used to rotate the 6" long vertical image into a horizontal one. The film writing speed was about 0.1 inch/micron.

III. EXPERIMENTAL PROCEDURE

a) Gas dynamic experiments: The driver was filled with 40 psig Oxygen and 240 psig Hydrogen. A 2000 psig diaphram was used to separate the driver from the driven section. In the driven section argon at 350 microns pressure was introduced. The driver mixture was ignited with an exploding wire, and the resultant shock velocity was measured by two 931 photo tubes placed four to five feet apart. The experiment was repeated for a 1500 psig diaphram with argon at 260 and 110 microns pressure.

b) Magnetic field measurements: With the tube at atmospheric pressure, the capacitor was charged to 10, 15, 10 KV and the spark gas was broken down. Measurements were made of the total current flowing in the coil and the magnetic field in the central region of the coil to determine its uniformity and strength.

c) Interaction of moving plasma with AC magnetic field: The plasma produced by the shock tube was passed through the field coil. When the front of the plasma was halfway inside the coil the field was turned on. The timing of this experiment is shown in Figure 1. It was accomplished by using a phototube to trigger the delay circuit of a 555 oscilloscope which broke down the spark gap through a thyratron and pulse transformer. When the capacitor discharged, it generated enough noise so that the phototube circuit was influenced by it. Thus it was possible to determine the position of the shock wave when the capacitor went off. Experiments were performed with the static gas pressure of the plasma behind the shock wave,

less than, equal to and greater than the magnetic pressure. The results were measured with search coils and observed with the smear camera. All the search coils measured the rate of change of the field dB/dt directly.

d) The "ring" discharge: With the 6" diameter tube filled with argon at 110, 260, 750 microns pressures, the field was turned on. The capacitor voltage was 15 and 19 KV. The resultant discharge was measured with search coils inside the tube and photographed with the smear camera. All the search coils measured dB/dt directly.

IV. EXPERIMENTAL RESULTS

The results will be listed in the same order as in the procedure.

A) Gas Dynamic Results:

The shock velocity, U_s, obtained in the gas dynamic experiments was between 4600 and 5300 MPS. This corresponds to a Mach number of 15 to 16.5.

A 6332 Photomultiplier showed that the rise in luminosity of the shocked gas occurred in a few microseconds. Petshek (9) and Gloersen (14) have observed that in argon and xenon shocks with a 1% impurity level that the gas behind the shock reaches thermodynamic equilibrium in a few microseconds. Since, 1% was the impurity level in this experiment one can use one dimensional shock tube theory (3) to compute the equilibrium properties of the gas behind the shock. The results are shown in Table I.

TABLE I
Computed Thermodynamic properties behind the shock wave

---	P_2	T_2	α_2	u_2	ρ_2
P_1 = 350 microns	0.16 atmospheres	11000°K	14%	$4.32\times10^5 \frac{cm}{sec}$	$6.05\times10^{-6} \frac{gm}{cc}$
P_1 = 260 microns	0.12 atmospheres	11000°K	16%	$4.34\times10^5 \frac{cm}{sec}$	$4.5\times10^{-6} \frac{gm}{cc}$
P_1 = 110 microns	0.069 atmospheres	11000°K	20%	$4.733\times10^5 \frac{cm}{sec}$	$2.45\times10^{-6} \frac{gm}{cc}$

The computed conductivity using the Spitzer formula (15) is 3700 mhos/m.

The uniformity of the properties of the gas behind the shock is determined by the radiation cooling of the gas behind the shock. Following Petshek's (9) analyses one

finds that the degree of ionization α decreases by 0.2% per cm behind the shock. Since the initial ionization is 14% one can conclude that the gas properties are uniform for at least 30 cm. This was confirmed by the 6332 phototube which showed that the light output of the gas was uniform for the entire slug length.

The length of the slug was measured by the time of luminosity recorded on the phototube. For P_1 = 350 and 260 microns it is 30 cm and for P_1 = 110 microns it is 110 cm. The slug length obtained at the higher pressures agrees with the computed theoretical slug lengths using formulas derived by Roshko (8). At the lower pressure the theoretical value is one half the experimental value of slug length.

B) Magnetic Field Measurements

With atmospheric air inside the shock tube, the field inside the shock tube was measured with magnetic probes. The measured field frequency was 67 KC and the logarithmic decrement was 0.223. This decay was sufficiently slow so that four useful field cycles could be obtained in each experiment. This time was equal to the testing time. The first half cycle peak values of the field were 1310 gauss, 1960 gauss and 2460 gauss for capacitor voltages of 10 KV, 15 KV and 10 KV.

The local field probes No. 5, 7 also showed that B was uniform and axial in the middle half of the solenoid and that it was of the same magnitude at the axis and wall of the shock tube.

An investigation (16) of the end effects of the field coil and the plasma led to the conclusion that they could be neglected in the region where the probes were located (Figure 2).

C) Interaction of a moving plasma with a high frequency magnetic field:

When the shock front of the plasma reached the center of the solenoid, the magnetic field was turned on. Magnetic probe No. 1 (Figure 2) showed that the presence of the plasma did not measurably reduce the total current in the solenoid. Probe No. 5 which was located on the outside wall of the shock tube, showed that the magnitude of B outside the plasma was unchanged by the presence of the plasma. Coil No. 4, which was wrapped around the shock tube, measured the total flux inside the shock tube well and the plasma. This measurement was recorded versus time on a 555 Tektronix oscilloscope. The shape of the oscilloscope traces was a damped sine wave. It was found that the percent reduction in the flux, ϕ/ϕ_o, (17), in the presence of the plasma, remained fairly constant (within 5%) during the time of the experiment (60 μ.sec.). To show the effect of the ratio of static plasma pressure to magnetic pressure on the flux reduction, the average value of ϕ/ϕ_o over one experimental run was plotted, versus the ratio of the static plasma pressure divided by the value of peak magnetic pressure in the first half cycle. This curve is shown in Figure 3. The values used for this curve are shown in Table II. The static plasma pressure in this table is taken from Table I. The letters A, B, C, etc., will be used to identify the various experiments. It can be seen from Figure 3, that for $P > B^2/\mu_o$, ϕ/ϕ_o has a constant value. As P becomes less than $B^2/2\mu_o$, ϕ/ϕ_o initially decreases and then increases. As will be shown in the discussion, this can be attributed to ohmic heating and magnetic compression.

Table II - Flux reduction ϕ/ϕ_o versus $P/B^2/2\mu_o$ for moving plasma experiment

	A	B	C	D	E	F	G
$P/B^2/2\mu_o$	2.3	1.7	.8	.55	.5	.47	.26
ϕ/ϕ_o	61%	61%	40%	50%	60%	50%	70%
P	0.16 atmos	0.16	0.12	0.16	0.12	0.069	0.069

To determine the concentration of the induced currents (i. e. $\vec{\nabla} \times \vec{B}$) inside the plasma, probe No. 7 was used (Figure 2). Measurements were made at r/r_o = 0.83, 0.67, and 0.33 (18). The voltage induced in the probe versus time was recorded on an oscilloscope. The shape of this curve was a damped sine wave. The % reduction in the amplitude of the field, B/B_o, inside the plasma, is reproduced in Figure 4.for experiment G and F. On the time scale axis, the testing time (or the length of the plasma slug) is shown. It will be noticed that as the probe enters and leaves the plasma, B/B_o is larger for a length equal to the skin depth of the field, δ , which is equal to 3 cm, (= 6 usec). The average value of B/B_o is shown in Table III for experiments, C, E, F and G.

Table III - Values of B/B_o at different positions r/r_o inside the plasma versus $P/B^2/2\mu_o$

	C	E	F	G	
P_{atm}	0.12 atmos	0.12	0.069	0.069	Theory
$P/B^2/2\mu_o$	0.8	0.5	0.47	0.26	

Table III - (continued)

Values of B/B_o					
$r/r_o = 0.83$	65%		60%	95%	74%
$r/r_o = 0.67$				40%	56%
$r/r_o = 0.33$	20%	20%	20%	20%	44%

The column marked "Theory" represents the computed values of B/B_o for an infinite solid cylinder with $r_o = 7.5$ cm, $\sigma = 3700$ mhos/meter in a 67 Kc field. This corresponds experimentally to the case $P \gg B^2/2\mu_o$. The data in Table III will be analyzed in the discussion.

The third set of observations was made with the smear camera. Figures 5a, b, c, show smear photographs of the vertical slit (Figure 2). These pictures correspond to experiments C, E, and G respectively. Point C corresponds to the case where $P = B^2/2\mu_o$ and the picture shows (Figure 5a) that there are no contractions at the edges, However, one can see bright horizontal strips at the edges which occur every 1/2 cycle of the field. This could be interpreted as heating of the gas which results in more luminosity. Points E and G correspond to the case where $P < B^2/2\mu_o$ and the camera shows periodic contractions (every half cycle) which become stronger as pressure decreases. The region of increased luminosity on the pictures is concentrated in a strip $1\frac{1}{2}$ cm thick. The smear photograph for experiment F is similar to experiment E, G.

The data of this section will be analyzed in the discussion.

D) The "Ring" Discharge Experiments

The results obtained in the "Ring" discharge experiments can be divided into two groups. One group consisted of experiments at high gas pressures and low magnetic field. The other group consisted of experiments at low pressure and high magnetic field. Representing the first group is the experiment with argon at 260 microns pressure and a peak field of 1460 gauss (corresponding to a 15 KV capacitor voltage). Representing the second group is the 100 micron, 2400 gauss (19 KV) experiment.

The highest pressure at which breakdown was obtained in our experiment was at 750 microns pressure and at a 1960 gauss peak field. This corresponds to an F/p of 30 V/cm/mm Hg at the outer edge of the gas. This is much lower than the minimum breakdown value which Blackman obtained in air, namely E/p = 1100. It is also much lower than the minimum breakdown of argon in a DC field; namely, E/p = 270 V/cm/mm Hg.

Ring discharge in argon at 260 microns pressure and 15 KV capacitor voltage: The peak value of E/p was 100 V/cm/mm Hg. Curve D in Figure 6 and Curve B and D in Figure 7 are a plot of the measurements made by Coil 4 and Coil 7 respectively. To understand the meaning of the curves one must examine the smear camera photograph (Figure 8a) which was taken in conjunction with these measurements. The smear camera photo shows four radial shocks with velocities of about 5×10^3 cm/sec. The shocks start at the outside edge of the gas every 7.6 microseconds. This is equal to the half period of the field. After 30 microseconds the luminosity extends to the wall.

With this photographic result one can understand Curve D in Figure 6 and Curves B and D in Figure 7. In the first half cycle the gas does not breakdown; therefore, both ϕ/ϕ_o and B/B_o are equal to 100%. The next four half cycles correspond to the radial shocks which are observed in the smear picture. Finally when the shock waves no longer appear one obtains a constant value of ϕ/ϕ_o = to 28% and B/B_o equal to 40% (at $r/r_o = 0.83$) and 10% (at $r/r_o = 0.33$)

In Figure 6 the curve labelled E is the computed value of the flux inside Coil 4 if the inside of the tube is filled with an infinite conductor (i. e. $\phi\,\phi_o$ = 22% represents the flux in the glass wall of the tube). This means that only 5% of the flux penetrates the plasma after 4 half cycles. Examination of Figure 7 also tends to confirm that most of the field is excluded from the plasma after 4 cycles, since B/B_o = 40% at $r/r_o = 0.83$. Therefore, the fields, and hence, the induced currents, are concentrated between $0.83 < r/r_o < 1.0$.

"Ring" discharge in argon at 100 microns pressure and 19 KV: The peak value of E/p was 500 V/cm/mm Hg. Figure 8b is a smear photograph of the experiment. One notices that the radial shocks last for the entire length of the experiment. The first shocks have velocities of 1.1×10^4 m/sec. Curve A in Figure 6 and Curve A, E, and F in Figure 9 are a plot of the measurements made by Coil 4 and Coil 7 respectively. Curve A of Figure 6 shows that ϕ/ϕ_o = 70% after two cycles. This is a much larger value than in the previous experiment. In Figure 9 values of B/B_o are shown for three different distances from the center. At $r/r_o = 0.83$ the final value of B/B_o = 70%;

at $r/r_o = 0.67$, $B/B_o = 18\%$, and at $r/r_o = 0.33$, $B/B_o = 10\%$. In this experiment one can see that the induced currents are mostly concentrated between $.67 < r/r_o < .83$. This result agrees with the flux measurement since ϕ/ϕ_o is larger.

"Ring" Discharge in Hydrogen: To show the importance of the speed of sound criteria (i. e. $a/2\pi R \ll f$) and also the difference between the "scylla" experiments of Bullis (6) and the argon experiments in this paper, a "ring" discharge was induced in Hydrogen at 100 microns Hg and with a 19 KV capacitor voltage.

The result is shown in the smear photograph in Figure 10. The radial shock velocity is 2.2×10^4 m/sec. One can also see that the hydrogen plasma travels to the axis of the tube and re-expands to the wall in every half cycle. This is similar to the result Bullis obtained.

V. DISCUSSION OF RESULTS

The analyses of the data will be divided into two parts: Part A will consider the results of passing a slug of gas dynamically heated argon through a magnetic field, and Part B will deal with the results of the ring discharge experiments.

Part A: Moving Plasma Interacting with Stationery, Time Varying Magnetic Field:

a) Interaction of Moving Plasma with the field for the Case $P > B^2/2\mu_o$: In this section the distribution of the 67 Kc magnetic field inside the moving plasma for the case $P > B^2/2\mu_o$ will be compared with the field distribution inside an infinite solid cylinder having the plasma radius, 7.5 cm, and conductivity σ = 3700 mhos/meter.

The general equation for the distribution of a magnetic field in the presence of a conductor moving with velocity $\vec{u}$ is given by (19)

$$\frac{\partial \vec{B}}{\partial t} = CURL(\vec{u} \times \vec{B}) + \frac{1}{\mu_0 \sigma} \nabla^2 \vec{B} \qquad (1)$$

The plasma in this experiment is moving in the axial direction. It was shown in Part IV B, that in the vicinity of the search coils, B is also axial. Hence, the curl term vanishes and Equation 1 becomes

$$\frac{\partial \vec{B}}{\partial t} = \frac{1}{\mu_0 \sigma} \nabla^2 \vec{B} \qquad (2)$$

This equation describes the behaviour of an alternating magnetic field in the interior of a conductor. The eddy currents induced by the field can be obtained from Maxwell's equation $\vec{\nabla} \times \vec{B} = \mu_0 \vec{J}$

The equation for the field inside an infinite cylinder is derived by McLachlan (20), for the case where both the fields and the axis of the cylinder are in the z direction. The result is:

$$B_z = B_0 \frac{M_0[p^{1/2} r]}{M_0[p^{1/2} r_0]} \exp j.[\omega t + \theta_0(p^{1/2} r) - \theta_0(p^{1/2} r_0)] \qquad (3)$$

Where B_0 is the magnitude of the external field, B_z is the value of the field at a distance r from the axis of the cylinder of radius, r_c, $p = i\omega\mu_0\sigma$, $M_0(p^{1/2}r)$ is the amplitude of the Bessel function $I_0[(ip)^{1/2}r]$, and $\Theta_0(p^{1/2}r)$ is the phase angle of the Bessel function $I_0[(ip)^{1/2}r]$. The values of these Bessel functions are tabulated by Dwight(21).

The radial distribution of the amplitude of B and the phase shift $[\Theta_0(p^{1/2}r) - \Theta_0(p^{1/2}r_c)]$ for an infinite cylinder with 15 cm diameter, σ = 3700 mhos/meter and f = 67 KC, are plotted in Figure 11, Curve A and B. These curves will be referred to later.

To compare the result of the above analyses with the measurements made in the experiment, the total flux inside the cylinder is needed. This is the flux that is measured by Coil 4 (see Figure 2). The total flux ϕ is:

$$\phi = \pi r_0^2 B_0\left[(2/p^{1/2}r_c)\frac{M_1(p^{1/2}r_c)}{M_0(p^{1/2}r_c)}\sin[\omega t + \Theta_1(p^{1/2}r_c) - \Theta_0(p^{1/2}r_c) - \frac{3\pi}{4}\right] + \pi(b^2 - r_c^2)B_0 \sin\omega t \qquad (4)$$

where r_c = 7.5 cm=plasma radius.
b = 8.7 cm = outside radius of the glass tube.

The second term represents the flux in the glass wall of the shock tube.

For the infinite cylinder one obtains a calculated value of ϕ/ϕ_0 = 65%, where ϕ_0 is the total flux with no conductor present. The measured values obtained for $p > B^2/2\mu_0$ as given in Table II and Figure 3 are 61%. This compares very well

with the calculated value and one can conclude that for the case where the field acts as a perturbation (i. e. $P \gg B^2/2\mu_o$) one can use the solid conductor eddy current theory to describe the electromagnetic effects.

b) Calculation of eddy current heating for the cases where the magnetic pressure is equal to, or greater than the gas pressure: It will be noticed that some experimental points in Table II and Figure 3 for which $P \leq B^2/2\mu_o$ show larger flux reductions ϕ/ϕ_o than the solid cylinder theory indicates. Part of this deviation can be accounted for by the heating of the gas through the induced eddy currents which raise the temperature and the conductivity, and, therefore results in a smaller value of ϕ/ϕ_o .

To obtain an estimate of this heating the infinite cylinder will again be used as a model. Using the techniques described in Smythe (13) or McLachlan (20) an expression can be derived for the time-averaged eddy current heating in a solid cylinder. It is

$$P_r = \frac{\pi B_o^2 \rho^{1/2} r}{\sigma \mu_o} \cdot \frac{M_0(\rho^{1/2} r) M_1(\rho^{1/2} r)}{M_o^2(\rho^{1/2} r_o)} \cos\left[\theta_1(\rho^{1/2} r) - \theta_o(\rho^{1/2} r) - \frac{\pi}{4}\right]\Bigg|_0^r$$

in watts/meter length of cylinder.

The above expression P_r still contains the variable r and must be evaluated between the limits zero and r, where $0 < r < r_o$ = radius of cylinder. At $r = 0$, $P_r = 0$, and at $r = r_o$, P_r equals P_{r_o}, the total eddy current power dissipated in the cylinder. In Figure 11, Curve C, the % of the power P_r dissipated between zero and r

divided by the total power, P_{r_o}, dissipated between zero and r_o, is plotted versus r/r_o for an infinite solid cylinder of radius r_o = 7.5 cm and σ = 3700 mhos/meter in a 67 Kc field. It can be seen that 50% of the heating is concentrated in the outer 1 cm and 75% of the heating is concentrated in the outer 2 cm of the cylinder.

If P_{r_o} is plotted versus σ at 67 Kc, one finds (16) that P_{r_o} reaches its maximum value at a conductivity slightly less than 3700 mhos/meter. As σ increases above 3700 mhos/meter, P_{r_o} decreases. However, the percent of the total heating concentrated in the outer one cm of the 7.5 radius cylinder stays the same. Therefore, the initial value of P_{r_o} at σ = 3700 mhos/M will be used to calculate the heating effect.

Using the above information, the temperature and conductivity rise in the outer 1 cm, due to eddy current heating, was calculated for experiments C to G (Table II). The compressibility of the plasma was neglected . In the calculation, the heating effect of the first field cycle (15.6 microsecond) only, was considered, because the logarithmic decrement of field is such that 50% of the heating of the first 6 cycles is dissipated in the first cycle. The most important assumption made was that the heating proceeds in thermodynamic equilibrium. Hence, the Saha equation can be used to calculate the final degree of ionization. This assumption will be discussed shortly.

The result of the calculations, using the above assumptions are given in Table IV. The letter C, D, etc. refer to the points in Table II.

Table IV

Eddy Current Heating of a Cylindrical Plasma

	C	D	E	F	G
$P/B^2/2\mu_o$	0.8	0.55	0.5	0.47	0.26
$P_{initial}$	0.12 atmos.	0.16	0.12	0.069	0.069
$T_{initial}$ (See Table I)	11000°K	----			
$\alpha_{initial}$ (See Table I)	16%	14%	16%	20%	20%
$\sigma_{initial}$	3700 mhos/m	----			
T_{final}	13000°K	13000°K	13800°K	13300°K	16000°K
α_{final}	47%	50%	57%	72%	95%
σ_{final}	5050 mhos/m	5070	4900	5400	6100

The final conditions in this table correspond to those in the outer 1 cm of the 7.5 cm radius plasma.

To relate the calculations of the preceeding paragraphs to the experimental data, the flux reduction ϕ/ϕ_o must be calculated for the above plasma cylinders. There are two conductivities in these cylinders: a) σ = 3700 mhos/meter for $0 < r/r_o < .83$, and b) σ = the values listed in Table IV under σ_{final} for $.83 < r/r_o < 1.0$. If one assumes that the entire cylinder has the final conductivity of Table IV then one should obtain the maximum possible flux reduction ϕ/ϕ_o. Curve D' in Fig. 12 is the plot of this ϕ/ϕ_o versus the ratio of magnetic to gas pressure. It can be seen that none of the experimental points, for which $B^2/2\mu_o \gg P$, fall on this curve. This result is not surprising for these experiments for which $P < B^2/2\mu_o$,

since they do not satisfy the initial assumption of the incompressibility of the plasma. The experiment for which $P = B^2/2\mu_o$ will be discussed in the next section.

c) Interaction of an a. c. field with a plasma satisfying the condition $P = B^2/2\mu_o$: Experiment C,(Table IV), does satisfy the incompressibility assumption (i. e. $P = B^2/2\mu_o$) yet the experimental value of ϕ/ϕ_o is 40% while the computed value is 59%. (Figure 12, Curve D').

One possible source of error lies in the assumption of thermodynamic equilibrium. If this is not correct then the Saha equation cannot be used to compute the final electron density. To justify the use of the Saha equation, one must show that the rate of ionization is sufficiently large that in the time of the heating (15 microseconds), the electron density approaches the value computed from the Saha equation. This computation was done (16) for all the experiments in Table IV assuming that the electrons have a Maxwellian distribution and that only electrons with energy greater than 15.7 volts can ionize the argon . It was found that for experiment C it takes 24 microseconds to reach the final equilibrium density. This is slightly longer than the heating time. However, argon has a metastable state at 11 volts and therefore, the ionization proceeds in two stages. One, excitation to 11 volts; two, ionization from 11 to 15 volts. Since there are more electrons in this region this ionization proceeds faster. Since the cross section for ionization from the metastable state is unknown the exact rate cannot be computed. But it seems reasonable to assume that the gas is in Saha equilibrium.

Another source of error was the assumption that the entire cylinder had the conductivity of the heated outer layer. To correct this one must solve the problem of a composite cylinder with two different conductivities, σ_1, σ_2, σ_1, is the conductivity of the unheated interior of the cylinder (i. e. 3700 mhos/meter) and σ_2 is the conductivity of the heated outer layer. A general solution was obtained (16) for the flux reduction ϕ/ϕ_o for a composite cylinder. The solution is a complicated combination of Bessel functions. An example was solved for the case where σ_2 = 5800 mhos/meter for 7.5 cm $\geq$ r $\geq$ 7 cm and σ = 3700 mhos/meter for $0 \leq r \leq 7$ cm. The values of ϕ/ϕ_o obtained is 44%. The solution for a solid cylinder with 7.5 cm radius and σ = 5800 mhos/meter gives ϕ/ϕ_o = 55% . One can thus see that a composite cylinder with two conductivities can have a greater flux reduction than a solid cylinder with one conductivity. This is an unexpected result. One would expect a solid cylinder of high conductivity to have a larger flux reduction than a composite cylinder, part of which has a low conductivity.

The reason for the larger flux reduction is due to the phase shift. It will be recalled that the value of B and ϕ inside the conductor consists of an amplitude and a phase. The phase of B is a function of radius (Figure 11, Curve B) and since ϕ is the integral of B over the area it is quite possible that the phases of B combine in such a way to reduce the total flux ϕ . The phase shift also reduces the total flux in a single conductivity cylinder. It is probably coincidental that in this experiment the conductivities at different radii in the plasma were such that a large flux reduction was obtained.

A third possible source of discrepancy between theory and observation arises from using the power distribution as shown in Figure 11, Curve C to calculate the heating of the plasma. It was assumed that the single conductivity cylinder solution can be used. However, as heating proceeds the conductivity of the outer layer of the plasma rises. Since an exact calculation of this effect is difficult, the smear photograph corresponding to this run will be used to estimate the region of heating concentration. Figure 5a shows very bright horizontal strips at the bottom edge of the film. The modulation of these strips is 1/2 cm. This would seem to indicate that the heating is more concentrated than was assumed in the last section. To obtain an upper limit on the heating effect, it was assumed that all the energy (22) of the first field cycle was dissipated in this 1/2 cm thick region. From this (16) one obtains σ = 9500 mhos/meter. Again assuming that the entire cylinder has a conductivity of 9500 mhos/meter, one finds that ϕ/ϕ_o is 49%. The experimental value of ϕ/ϕ_o = 40%. It can be thus seen that this equilibrium heating calculation does account for a large part of the flux reduction observed.

Upon examination of the measurements of the probe (No. 7) inside the plasma (See Table III) one finds that it agrees with the smear photograph.

Table V compares the values obtained experimentally, with the theoretical values for solid cylinders with σ = 3700 mhos/meter and σ = 9500 mhos/meter. σ = 3700 mhos/meter represents the plasma conductivity before the magnetic field is turned on . σ = 9500 mhos/meter corresponds to the conductivity computed in the previous paragraph.

Table V: Comparison of experimental measurements of local magnetic field inside the plasma with the corresponding theoretical values in an infinite cylinder of conductivities σ = 3700 and 9500 mhos/meter.

Position of the Probe No. 7	σ = 3700 mhos/m	σ = 9500 mhos/m	Exp. points
r/r_o = .83	74%	58%	65%
r/r_o = .33	44%	15%	20%

From this table one can see that at $r/r_o = 0.33$ the agreement between experimental and theory is good if one assumes a high conductivity of 9500 mhos/meter. This clearly indicates that the plasma is heated by the magnetic field.

As a result of the smear photography and local field probe No. 7 one can see that the probable reason for the large flux reduction, ϕ/ϕ_o, measured by coil 4, is due to intense heating at the outer edge of the plasma. As discussed previously, this heating is due to a complicated distribution of eddy currents which the simple eddy current theory does not predict.

The phase shift effect is secondary in causing a large flux reduction, since it was found (16) that it did not agree with the local field probe measurements near the axis of the plasma.

d) Interaction of an a. c. field with a moving plasma satisfying the condition $P < B^2/2\mu_o$:

In section (b) the heating effect was calculated neglecting compression. The result of this computation was plotted as Curve D' in Figure 12. However, the smear camera photographs, (Figure 4b, c) corresponding to these runs for which $P < B^2/2\mu_o$ show periodic contraction of the plasma.

A simple way to correct $\emptyset$ for the compression of the plasma (whose initial radius $r_o = 7.5$ cm) is to recompute curve D' in Figure 12 keeping the 8.75 cm radius of the measuring Coil 4 fixed and decreasing the radius of the plasma cylinder. The result of this computation is shown in Figure 12, Curve C', B', and A'. Curve C' represents the theoretical flux measured by Coil 4 when the plasma has a radius of 7 cm, Curve B' and A' correspond to the plasma radii of 6.5 and 6 cm respectively. It can be seen that none of the experimental points for which $P < B^2/2\mu_o$ fall on these four curves. This shows that the heating theory developed in section B is not in agreement with experimental observations. This was already demonstrated for the case $P = B^2/2\mu_o$ in section (c).

A better determination of the amount of compression of the plasma can be made if one uses an experimental value of the amount of flux the plasma excludes when it is heated, but not compressed (i. e. when $P = B^2/2\mu_o$). The difference between the actual value of $\emptyset$ measured when $P < B^2/2\mu_o$ and the value of $\emptyset$ measured for this case (i. e. $P = B^2/2\mu_o$) represents the amount the plasma is compressed. From this one can compute the final radius of the compressed plasma.

The result of this calculation is shown in Table VI. The first three lines are identical with Table III.

Table VI: Amount of Compression of Plasma by the Field using experiment C as the standard plasma flux exclusion

	C	D	E	F	G
$P/B^2/2\mu_o$	1.0	0.55	0.5	0.47	0.26
P (atmospheres)	0.12	0.16	0.12	0.069	0.069
ϕ / ϕ_o	40%	50%	60%	50%	70%
Computed plasma radius	7.5 cm	7 cm	6.75 cm	7 cm	6.2 cm

It can be seen from Table VI that a contraction of the radius less than 1.3 cm accounts for the measured flux reduction. This result can be checked by the smear photographs.

The smear photographs Figure 5a, b, c, corresponding to experiments C, D, and G respectively show that the contradictions increase with increasing values of $B^2/2\mu_o$ and they vary from zero to 1.5 cm. One can thus conclude that the method of using experiment C as a standard gives fairly accurate results of the amount of plasma contraction.

Another way to test the confinement of the plasma by the magnetic field is by using local magnetic probe (No. 7 in Figure 2) inside the plasma. The basis of this test is as follows: the eddy currents, $\vec{J}$, induced by the time varying applied magnetic field, produce opposing magnetic fields determined by the expression $\mu_o \vec{J} = \vec{\nabla} \times \vec{B}$. Due to these secondary fields, the depth of penetration of the applied field is of the order of the skin depth, δ, in the conductor. Hence,

by measuring the peak concentration of the field inside the plasma one can determine where the currents are flowing. If this peak concentration of $\vec{\nabla} \times \vec{B}$ is some distance, A, away from the wall, one can conclude that in the region A there exists no conducting plasma, otherwise currents would flow there. However, there may be nonconducting gas in this region. In this experiment the plasma is highly ionized, therefore, if the concentration of $\vec{\nabla} \times \vec{B}$ is a certain distance away from the wall the plasma is probably contained. As an example, the results of experiment F and G will be used. The experimental values of B for these two cases were tabulated in Table III and were plotted in Figure 4. In Figure 4, Curve A shows that for experiment G ($P/B^2/2\mu_o = 0.26$) at $r/r_o = 0.83$, (i. e. at 1.3 cm from wall), $B/B_o \cong$ 100 % while Curve D shows that for experiment F ($P/B^2/2\mu_o = 0.47$) at $r/r_o = 0.83$, $B/B_o = 60\%$. One can, therefore, conclude that the outer boundary of the conducting plasma has moved away from the wall as the magnetic field pressure was increased. From Curve A one can conclude that the plasma has been pushed at least 1.3 cm from the wall when $P/B^2/2\mu_o = 0.26$. This result agrees with the smear camera, Figure 5c, and the total flux observation Table VI, experiment G.

In section (b) of this chapter a simple theory was used to estimate the heating of the gas. For experiment G (i. e. $P/B^2/2\mu_o = 0.26$) the calculated temperature, degree of ionization and conductivity were 16000°K, 95% and 6100 mhos/meter respectively. The local measurements of the field can be used to estimate the error of this analyses.

Figure 4 shows that for $r/r_o = 0.83$, $B/B_o = 95\%$ (Curve A) and for $r/r_o = 0.66$, $B/B_o = 40\%$ (Curve E) . A conductivity of $\sigma = 14500$ mhos/meter will give the observed field reduction. This corresponds to a temperature of 27000°K. To heat the plasma to this temperature in thermodynamic equilibrium would require double ionization of the plasma. A computation was made (16) which showed that the ionization time for double ionization was longer than the testing time. Hence, one can conclude that only the electrons are at 27000°K but the plasma is at a lower temperature.

It is interesting to note that, although the magnetic pressure is four time the gas pressure, the gas is not pushed more than 1.3 cm from the wall in experiment G (Figure 5c). The reason for this is as follows: the gas has a dynamic pressure in the axial direction which is twice the magnetic field pressure. Behind the radial magnetically induced shock the gas pressure equals the magnetic pressure. The magnetically heated gas, therefore, acts as a boundary between the undisturbed flow and the wall. As this cylindrical boundary contracts the effect is similar to a supersonic diffusor. To calculate the effect of the contraction of the boundary, on the undisturbed flow, one can use the one dimensional supersonic flow theory. The Mach number of the plasma before the field is turned on is 2.8. Since it is ionized strongly, the ratio of specific heats is about 1.1. From the smear photograph one can see that the gas is pushed in at the walls about 1 cm. This reduces the undisturbed cross sectional area of the flow by 25%. Using the one dimensional gas tables

for $\gamma = 1.1$ one finds the new Mach number is 2.62 and the new static pressure is 1.5 times the original one. One can see that this effect does raise the pressure in front of the magnetically driven gas as it tries to penetrate into the interior of the moving plasma.

Due to this dynamic pressure effect, the plasma is not compressed more than $1\frac{1}{2}$ cm from the walls. It is, therefore, difficult to determine whether the plasma can reexpand to the wall each half field cycle. However, from the experiment one can conclude that if the boundary of the container were suddenly removed that the plasma would be contained by the field. This is due to the fact that the plasma can only expand at the speed of sound and during the time in each cycle of the field when $B^2/2\mu_o$ is less than the plasma pressure, the plasma can expand less than a centimeter in our experiments.

Part B: Discussion of Ring Discharge Experiments:

a) Breakdown Values of E/P: In Section (d) of the Experimental Results it was observed that in our experiments the value of E/P required for breakdown is much lower than that reported in Blackman (5) and it is also lower than the D. C. breakdown value in argon. It must be noted that Blackman's results agree only qualitatively with the D. C. Paschen Curves. As stated in the introduction no accurate data exists on the breakdown fields in a. c. "ring" discharges. This is due to improper electrostatic shielding of the solenoids used. In the Scylla experiments no experiments were performed to determine the minimum breakdown voltage. Therefore, no conclusion will be drawn concerning the breakdown voltages obtained in this experiment.

b) Discussion of "Ring" Discharge in Argon at 260 microns pressure and 15 KV Capacitor Voltage: Before discussing the results a qualitative description of the various phenomena occuring in this experiment will be given. During the first half cycle ionization by the induced electric field builds up the electron density sufficiently so that on the second half cycle the gas breaks down at its outer surface. The instant after breakdown the gas consists of cold (Room Temperature) neutrals and ions, and hot electrons (T_e equals 1 e. v. to 10 e. v.) . This phenomena is called a "ring" discharge. The interior of the gas cylinder is unaffected by this process. However, as the magnetic field amplitude rises, it exerts a pressure $B^2/2\mu_o$ on the conducting ring and forces it toward the center. In this experiment $B^2/2\mu_o/P$ = 400 therefore a strong radial shock is formed. This process of breakdown followed

by radial shocks will continue until the gas pressure in the tube equals the magnetic pressure. There are therefore, two processes occuring successively:

1) Ionization and breakdown by the induced electric field at the edge of the gas. This process causes electric field ionization.

2) Magnetic shocks which heat the neutrals and ions and raise the gas pressure. This process causes thermal ionization.

With this introduction the data will now be discussed. In order to determine the electron density and electron temperature at the instant of breakdown, experimental values of the ionization frequency and electron distribution are needed. The only such data exists for microwave discharges where the electron density is 10^{-6} times the gas density. Hence these results cannot be applied to a high density discharge as is the case in this experiment.

However, the magnetic probes can be used to determine the average conductivity and hence the average electron temperature over a cycle of the plasma. This conductivity is the result of both electric field ionization and thermal ionization by the magnetically driven shocks. The results of the smear photographs can be used to determine approximately the neutral and ion temperature, the thermal degree of ionization and the plasma pressure behind the magnetically driven shocks.

The smear photograph shows that there are four radial shocks spaced 7.5 microsec. (1/2 field cycle) apart. At the start of the following half cycle the luminosity fills the entire tube. The velocity of the four shocks is approximately equal.

The first shock has a velocity of 4.7×10^5 cm/sec. Using one dimensional shock tube theory and assuming thermal equilibrium ionization behind the shock one finds T = 10500°K, α = 12% and p = 0.12 atmospheres. This pressure is equal to the peak magnetic pressure. The second shock starts 7.5 microseconds after the first one. The mechanism is again the same as in the first shock, the electric field breaks down the gas and the magnetic field shock compresses it. A simple entropy argument can be used to show that the gas in front of the second shock has a lower density than the gas in front of the first shock. This gas probably consists of hot neutrals left behind the first shock.

Once the shocks have stopped, at the start of the sixth half field cycle, probe No. 7 (Figure 7) indicates that the bulk of the field in the gas is concentrated in the region between the wall and 2 cm away from the wall. Probe No. 4 (Figure 6), which measures the total flux inside the shock tube, indicates that approximately 5% of the flux penetrates the gas. To estimate the conductivity one can use the simple one-dimensional eddy current theory since the curvature of the thin 2 cm thick layer of plasma is not important in such a thin region.

Solving the equation $\frac{\partial \vec{B}}{\partial t} = \frac{1}{\mu_0 \sigma} \nabla^2 \vec{B}$ for the one-dimensional case, one finds $B_z = A e^{-z/\delta} + C e^{+z/\delta}$ where A, C are constants, δ is the skin depth and z is the distance from the edge of plasma to the point z inside the plasma. The boundary conditions are at $z = 0$, $B = B_0$ and $z = 2$ cm, $B = 0$. This assumption is based on the Probe No. 7 measurements. One finds that $A >> C$.

$$\therefore B_z = B_0 e^{-z/\delta} \cos(\omega t - z/\delta)$$

where δ is the skin depth.

$$\phi = \int_0^{2\,cm} B_z \, dz = \frac{1}{\sqrt{\delta}} B_0$$

If one assumes a σ of 10^5 mhos/meter one computes $\phi/\phi_0 = 6.2\%$. This is the total flux penetration inside the plasma at 260 microns initial pressure. It compares very well with the 5% measured. (Note: the effect of the glass wall is 22% and in Figure 6 this must be added to the 5%). For a $\sigma = 10^5$ mhos/M one obtains a temperature of 90,000°K. It is obvious that the ions are not heated to these temperatures because the field does not have enough energy to do this. Therefore, this is the temperature of the electrons.

The search coils clearly indicate that the conductivity of the plasma is much higher than in the moving plasma experiments, and that the electrons are a much higher temperature than the gas temperature. In the moving plasma experiment $T_e = T$ gas. To understand the difference between this result and the eddy current heating in the moving plasma experiments we must consider the way in which the plasma is heated. In the moving plasma experiments, the electrons have initially a Maxwellian distribution and it was shown that the eddy current heating initially proceeds in equilibrium. In addition, there was no breakdown each half cycle be-

cause E/P was about 1 Volt/cm/mm Hg. In this experiment the electrons are produced by a breakdown mechanism and it is unlikely that initially they have a Maxwellian distribution. Without experimental knowledge of the ionization frequency it is impossible to say anything about the temperature and distribution of the electrons. However, one can say that since the gas is highly ionized it will rapidly assume a Maxwellian distribution. When this occurs, the ionization frequency at 90,000°K of both the first and second ionization level in argon will be high enough to doubly ionize the gas in a few microseconds. This will result in a very rapid lowering of the electron temperature. In other words, the high temperature in this experiment is only a transient.

It is interesting to compare this result with the one obtained in a steady state "ring" discharge with no shock waves (i. e. where $B^2/2\mu_o = P$). Cabannes (23) performed experiments with steady state "ring" discharges in argon, at pressures of 0.1 to 10 mm Hg with a 1 Mc field. His results were as follows: the eddy current power input was less than 1 KW. [redacted] was 1 Volt/cm/mm Hg. The degree of ionization was between 1 and 10% and the measured electron temperature was 28000°K (≈ 3 e.v.).

Pistunovich (24) performed an electrodeless discharge experiment in a toroidal chamber with D_2 at 0.4 mm Hg pressure, using a 25 KV capacitor bank to initiate the discharge. The capacitor circuit was critically damped and the discharge lasted

a few hundred microseconds. By using a double floating probe he measured an electron temperature of about 5 e. v. and a degree of ionization of 3 to 10% depending on the initial voltage of the capacitor. The results of these experiments seem to indicate that in our experiments the high electron temperature is only a transient effect. It is also interesting to note that Cabannes' result is similar to the moving plasma experiment G (see Discussion Part A, section d). Therefore, it would seem that once a steady state is reached the ring discharge, the plasma will have the same properties as the moving shock heated plasma. This equivalence will be demonstrated in the next section.

c) "Ring" discharge in argon at 100 microns pressure and 19 KV: The major differences in the experimental results between the 100 micron and 260 micron experiment were outlined in Section D of the "Experimental Results" section. These will now be discussed.

The value of E/P was 500 V/cm/mm Hg. One would, therefore, expect a larger degree of ionization at breakdown. This fact coupled with the larger ratio of magnetic pressure to gas pressure of approximately 3000, accounts for the stronger radial shocks in this experiment. (Figure 8b). In addition, the smear photograph (Figure 8b) shows that the shock pattern extends for about 8 half cycles. This is approximately equal to the useful testing time in this experiment. The velocity of the first two radial shocks is 1.1×10^6 cm/sec. Using one-dimensional shock theory one finds the temperature behind the first shock is 16,000°K and the degree of

thermal ionization. is 90% . The one-dimensional shock theory is useful only in estimating the gas temperature. However, the degree of ionization of 90% is probably inaccurate since it is not certain how fast equilibrium ionization is established behind the shock. In addition, the contribution to the electron density due to electric field ionization cannot be estimated. The static pressure behind the shock can be obtained roughly from $P_2 = \rho_1 U_s^2$, where ρ_1 = the gas density at 100 microns and U_s the shock velocity. From this one obtains, P_2 = .24 atmospheres. This pressure is the same as the maximum magnetic pressure. The second shock has the same strength as the first shock, therefore, the static pressure behind the second shock, P_3, is only slightly less than the static pressure after the first shock, P_2. Using this information, and remembering that for conservation of momentum $P_3 = \rho_2 U_s^2$ one finds the density, ρ_2, in front of the second shock is about $.175 \times 10^{-6}$ gm/cc. This is 4% of the density behind the first shock and 80% of the density ahead of the first shock. Now, the gas behind the first shock clearly did not have enough time to re-expand to the wall after the field started to decrease from its peak value for two reasons. One, it can only expand at the speed of sound, which is 20% of the inward velocity; and two, the smear picture shows that the first shock has not reached the ends of the tube when the second one starts. Thus the particles through which the second shock wave travels consists of neutral gas atoms which diffused through the magnetic field behind the first shock. The temperature of these neutrals is definitely higher than room tempera-

ture because one shock wave has passed through it and therefore, its entropy rose. With each successive shock the density near the wall of these neutral atoms decreases due to electric field ionization followed by magnetic compression. Therefore, in a steady state the entire plasma should be contained by the magnetic field.

The fourth and all successive shocks have nearly the same velocity $v = 4.8 \times 10^6$ cm/sec. This gives a density in front of the shock (from $\rho U^2 = p$) of 2.4×10^{-6} gm/c.c. This is the same value as the density of the shock heated gas behind the first few shocks. In other words, from the fourth shock onward, the central region of the tube is filled with shock heated plasma; whose pressure is of the order of the magnetic pressure. This explains why the compression of the plasma is less than in the previous cycles. It is reasonable to conclude that after the fourth shock the experiment approaches a steady state, with the bulk of the plasma confined away from the wall. The additional shocks ionize and compress any neutral gas which leaked across the field toward the wall.

Upon examining the data obtained from the search coils (Figure 6 and 9) one is led to the same conclusions as were reached above (i. e. that the plasma is confined by the field).

Figure 6, Curve A, shows that $\emptyset/\emptyset_o$ is larger than in the 260 micron experiment, thus indicating that more flux has penetrated the glass tube. Figure 9, Curves A and E show that the field concentration in the tube is located between $r/r_o = 0.83$ and $r/r_o = 0.66$. This also tends to indicate that the edge of the plasma cylinder is in the vicinity of $r/r_o = 0.83$.

An interesting result is that the data from the search coils 4 and 7 (Figures 6 and 9) is similar to the data obtained for the moving plasma experiment G (i.e. $P/B^2/2\mu_o$ = 0.26) (see Table II, III). In Experiment G it was concluded that the plasma was contained and that the outer surface of the plasma was at least 1.3 cm from the wall. Both this experiment and Experiment G have a flux reduction ϕ/ϕ_o = 70% (Table II and Figure 6, Curve A). In addition, the local field distribution in this experiment (Figure 9) shows that at r/r_o = 0.83, B/B_o = 70% (Curve A) while at r/r_o = 0.66, B/B_o = 20% (Curve E). The difference between these two readings is 50%. The corresponding differences between the field readings at the same position is 55% in Experiment G. (Figure 4) From this one can conclude the following : a) the electron temperature, and hence the conductivity, are lower in this experiment than in the ring discharge experiment at 260 microns. The lower electron temperature is due to the fact that this experiment has stronger shock waves. Hence, the hot electrons are pushed into the interior of the gas where they rapidly loose their energy in ionizing collisions with neutral argon atoms. b) that steady state containment has been obtained in the 100 micron ring discharge experiment. c) that magnetic containment of a steady state ring discharge is similar to magnetic containment of a moving plasma. d) the conductivity near the edge of the plasma in this experiment is similar to the one obtained in experiment G (i. e. 14500 mhos/ meter.)

d) <u>"Ring" discharge in hydrogen -</u> In the experimental results section (d) it was reported that in hydrogen, the shock wave travels to the axis of the tube in 1/4 cycle

and is reflected to the wall in 1/4 cycle. The measured shock velocity is 2.2×10^4 cm/sec. This velocity equals the magnetic "field velocity" (i. e. the rise time of the field) R/τ, where R = 7.5 cm and τ = 67 Kc. It is thus seen that the hydrogen plasma is not continuously contained by the field. To prove this the temperature and speed of sound behind the shock was calculated using one-dimensional shock theory. It was found, assuming thermodynamic equilibrium, that T = 11,500°K and $a = 10^6$ cm/sec. Hence, $a/4\pi R$ = 10 Kc. Since this is only 6.5 times less than the field frequency it does not satisfy Butler's third a. c. containment criteria (i. e. $a/2\pi D \ll \tau$). One can, therefore, see that even if $\delta \ll R$ as it is in the hydrogen experiment, one does not obtain a. c. containment if $a/2\pi D \geq \tau$.

The shock pattern obtained in the hydrogen experiment is similar to the one obtained by Bullis (6).

VI. CONCLUSIONS

A) Moving plasma interacting with a time varying field

1) $P > B^2/2\mu_o$

For this case the eddy current theory of a solid cylinder in a uniform time varying magnetic field gave good agreement between the theoretical flux reduction, ϕ/ϕ_o = 65%, and the measured flux reduction, ϕ/ϕ_o = 60%, if one used the initial plasma conductivity of 3700 mhos/m. This conductivity was computed from the equilibrium plasma temperature. From this one can conclude:

a) there were no gas dynamic effects due to the field

b) the entire plasma cylinder had a uniform temperature and conductivity

c) the skin depth, δ, was less than the plasma radius, hence Butler's containment criteria $\delta < R$ was satisfied for all the moving plasma experiments.

2) $P = B^2/2\mu_o$: In this case the measured flux reduction was lower than the value predicted by the eddy current theory for a solid conductor. This deviation was attributed to heating of the outer layer of the gas by the induced eddy currents, which resulted in a higher gas conductivity. It was concluded that the large flux reduction measured, was due to distribution of eddy currents, near the edge of the plasma, which cannot be computed by the eddy current used in this paper. A secondary cause of the large flux reduction could be due to the fact that the phases of the field

in regions of the gas with different conductivities, cancel each other in such a way as to reduce the total flux.

3) $P < B^2/2\mu_o$: Based on measurements of the total flux in the shock tube it was concluded that due to magnetic compression, the radius of the plasma was reduced by about one cm in these experiments. This amount of compression was also observed on the smear photograph, and by the magnetic probe inside the plasma. The magnetic probe showed that the field (and hence, the induced current) concentration was between 1 and $2\frac{1}{2}$ cm away from the wall for Experiment G. Therefore, it was concluded that there was no conducting gas in this region and since the plasma was highly ionized, it was concluded that a large percentage of the plasma was contained by the magnetic field. It was also shown that a supersonic diffusor effect accounted for the amount of compression of the plasma.

Since the plasma in this experiment satisfies both of Butler's containment criteria (i. e. $\delta < R$ and $a/2\pi D \ll \ell$) one can conclude that a high frequency field can be used to remove a low temperature (10000°K) plasma from a material wall.

B) Ring Discharge in argon at 260 and 110 microns initial pressure

The overall characteristics of the ring discharge experiments were similar to those obtained by Bullis (6) and Blackman (5). The following differences were observed.

1) The minimum value of E/p for which breakdown occurred was by an order

of magnitude less than the minimum E/p obtained from the D. C. Paschen Curve.

2) In the 260 micron experiments the smear photograph showed that the plasma extended to the tube wall at the start of the sixth half field cycle. Based on measurements of the previous shock velocities the gas temperature was estimated in the order of 10,000°K. Based on magnetic probe measurements it was concluded that the electron temperature was about 90,000°K. Cabannes (23) and Pistunovich (24) obtained in steady state ring discharge experiments, electron temperatures of about 30,000°K and 50,000°K, respectively. It was, therefore, concluded that the high electron temperature in our experiment was only transient phenomena and that once a steady state is established, the electron temperature would drop sharply due to ionizing collisions of electrons with atoms.

3) In the 100 micron experiment it was concluded that after three radial shocks the main body of the plasma is confined in the central region of the glass tube away from the wall. This was confirmed by means of a magnetic probe, inside the glass tube, which showed that the current concentration, and hence the edge of the plasma, was situated between $1\frac{1}{2}$ and $2\frac{1}{2}$ cm away from the wall.

Based on the smear photograph which showed that radial shocks originated at the wall each half cycle, it was concluded that any neutral atoms which remained outside the main plasma body would be ionized by the induced electric field and compressed into the main plasma body by the magnetic field.

From the magnetic probe measurements the electron temperature was estimated at 3 e. v. From this one can conclude that the 10 e. v. electron temperature obtained in the 260 micron experiment was only a transient phenomena.

The most interesting result was that the boundary of the plasma and the conductivity of the outer layer of the plasma as measured by the probes for the 110 micron experiment was about the same as Experiment G (i. e. $B/B^2/2\mu_o = 0.26$) of the moving plasma experiments. From this one can conclude that in this ring discharge experiment the plasma conditions are such that they satisfy Butler's containment criteria (1).

C. Ring discharge in hydrogen

In this experiment $a/2\pi D$ was about 1/5 the field frequency, hence, the hydrogen plasma did not satisfy Butler's containment criteria. It was concluded that this was the reason why the plasma was able to re-expand to the wall each half cycle, (i. e. the plasma was not continuously confined by the field as in the argon experiments). This result is similar to the early Scylla experiments of Bullis (6).

D. General conclusions

From the above experiments it can be seen that if $a/2\pi D \ll f$ one can obtain magnetic confinement of the plasma. It was concluded that in Experiment G ($P/B^2/2\mu_o = 0.26$) of the moving plasma experiment and in the 100 micron "Ring"

discharge experiment in argon the ionized portion of the gas was confined by the magnetic field. The basis for this conclusion was the local magnetic probe measurement which showed that the induced currents in the gas were concentrated between $1\frac{1}{2}$ and $2\frac{1}{2}$ cm away from the wall. It is very probable that some unionized gas was at all times in contact with the wall. Since the argon gas near the wall was highly ionized due to ohmic heating by the field and electric field ionization the density of un-ionized gas in contact with the wall was probably small.

Footnotes:

* Based on a thesis submitted to M. I. T. for the degree of Doctor of Science.

Now at Space Sciences Laboratory, General Electric Company, Valley Forge, Pennsylvania.

1) J. W. Butler, A. J. Hutch, and A. J. Ulrich, "Proceedings 2nd International Conference on the Peaceful Uses of Atomic Energy" (United Nations Publications, Geneva 1958) Vol. 32, p.

2) L. Aamodt and S. Colgate, "Nucleonics", 15, 50 (1957).

3) E. L. Resler, S. C. Lin, and A. Kantrowitz, "J. Appl. Phys. " 23, 1390 (1952)

4) G. F. Francis, "Ionization Phenomena in Gases", (Academic Press, New York 1960) p . 137

5) V. Blackman and B. Niblett, "The Plasma in a Magnetic Field", R. Landshoff, ed., (Stanford University Press, Stanford 1958).

6) W. H. Bullis, TID 7536 Pt. II (U. S. Atomic Energy Commission, Washington, D. C.)

7) R. E. Duft, Phys. Fluids 2, 207 (1959)

8) A. Roshko, Phys. Fluids 3, 835 (1960)

9) H. Petschek and S. Byron, Ann. Phys. N. Y. 1 , 270 (1957)

10) S. C. Lin, E. L. Resler, and A. Kantrowitz, J. Appl. Phys. 26, 95 (1955)

11) H. E. Petschek, P. H. Rose, H. S. Glick, A. Kane and A. Kantrowitz, J. Appl. Phys. 26 , 83 (1955)

12) The field coil is such that the volume of the coil should be large compared to the plasma volume. By choosing a 14" coil diameter it was found that one could obtain an 8 cycle ringing time. In addition the coil was made long enough to produce a uniform axial field in the middle half of the coil. The coil calculations follow the method outlined by Butler (see footnote 1) and Smythe (see footnote 13).

13) W. R. Smythe, "Static and Dynamic Electricity", (McGraw Hill, Inc., New York, 1950) 2nd Ed., Chapt. 7, 9, 11.

14) P. Gloersen, Phys. Fluids 3 , 857 (1960).

15) L. Spitzer, "The Physics of Fully Ionized Gases", (Interscience Publications, Inc., New York 1958).

16) B. Zauderer, Sc. D. Thesis in Mechanical Engineering, Massachusetts Institute of Technology, Cambridge, Massachusetts, 1961.

17) ϕ_o represents the total flux in the shock tube (including the glass wall) with no plasma present.

18) $\mathcal{R}_o$ is the I. D. of the shock tube of 7.5 cm.

19) T. G. Cowling, "Magnetohydrodynamics", (Interscience Publications, Inc., New York 1957), p. 3.

20) N. W. McLachlan, "Bessel Functions for Engineers"(Oxford University Press, London 1934, Chapt. 9).

21) H. B. Dwight, "Mathematical Tables", (Dover Publications, Inc., New York 1958).

22) P_r has its maximum value at σ = 3700 Mhos/m for a fixed 67 K. C. field and P for a fixed 7.5 cm radius cylinder. It is this value of P_{r_o} that was used in the calculations.

23) F. Cabannes, Ann. Phys., Paris, 10 , 1026 (1957).

24) V. I. Pistunovich, "Measurement of Electron Temperatures and Ion Concentration by a Double Floating Probe in an Electrodeless Discharge", in Plasma Physics and Controlled Thermonuclear Reaction" , Leontovich Ed. (Pergamon Press, London, 196) Vol. IV, p. 157).

Acknowledgement

The author is indebted to Dr. J. A. Fay for his aid in the conduct of this work. He wishes to thank his colleagues, especially Mr. Arthur Schneiderman and Mr. Kenneth Rathjen for their help with the experiments. This work was supported in part by the National Sciences Foundation, the United States Air Force Cambridge Research Center, and by Project "Squid", Office of Naval Research.

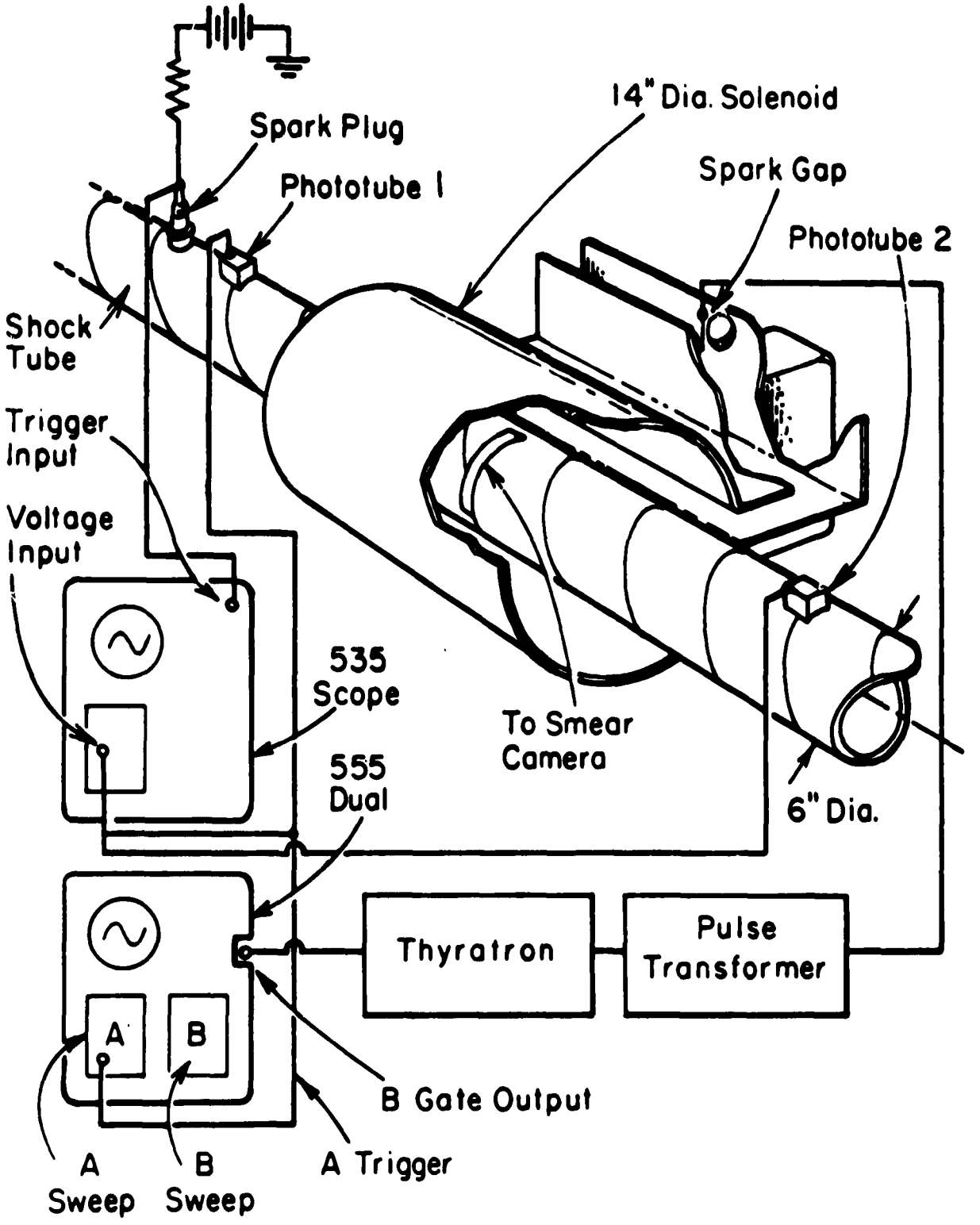

Figure 1. Schematic Diagram Showing the Moving Plasma Experiments, Test Section, Including the Instrumentation Used. The Left Side of the Diagram Represents the Upstream End of the Shock Tube. The 535 Tektronix Oscilloscope Measured the Shock Velocity. The 555 Duel Beam Oscilloscope Triggered the Field Coil Circuit Through the "A Sweep" Time Base. The "B Sweep" Time Base was Used for the Magnetic Probe Measurements.

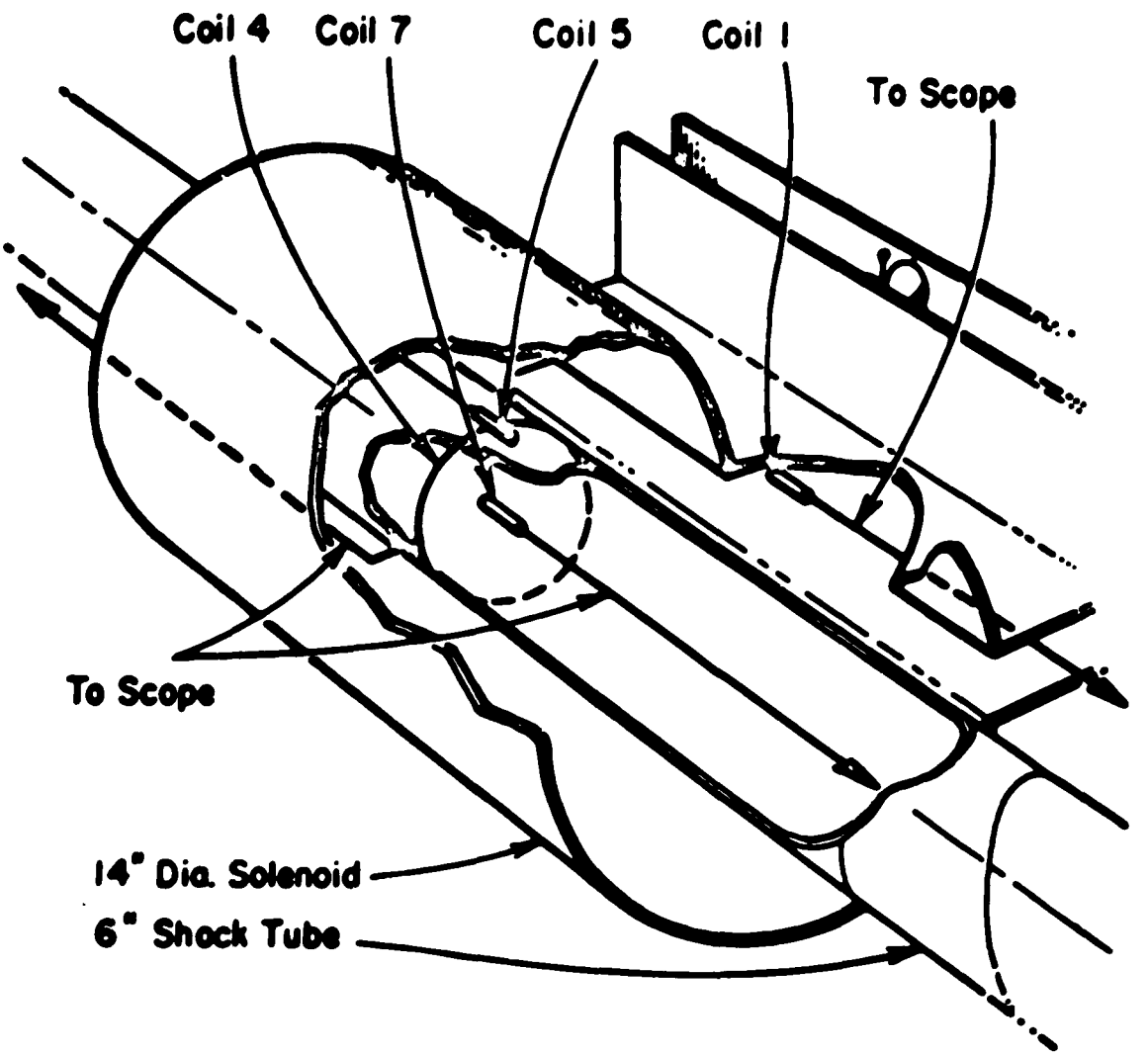

Figure 2. Schematic Diagram Showing the Location of the Magnetic Probes.

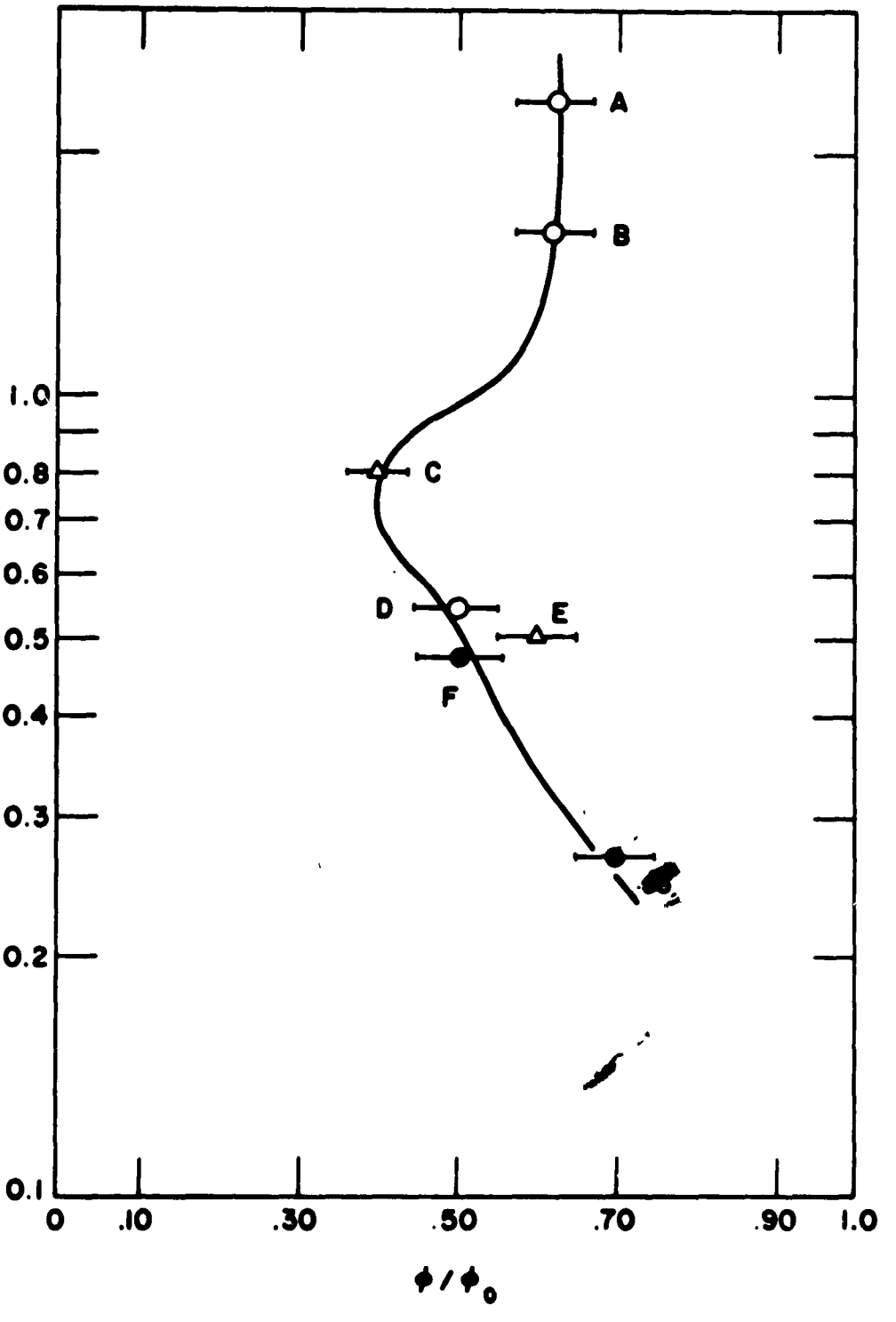

Figure 3. Average Flux Reduction, ϕ/ϕ_o, (as Measured by Probe No. 4) Versus $P/B^2/2\mu_o$ for the Moving Plasma Experiments. These Experimental Points are Tabulated in Table II.

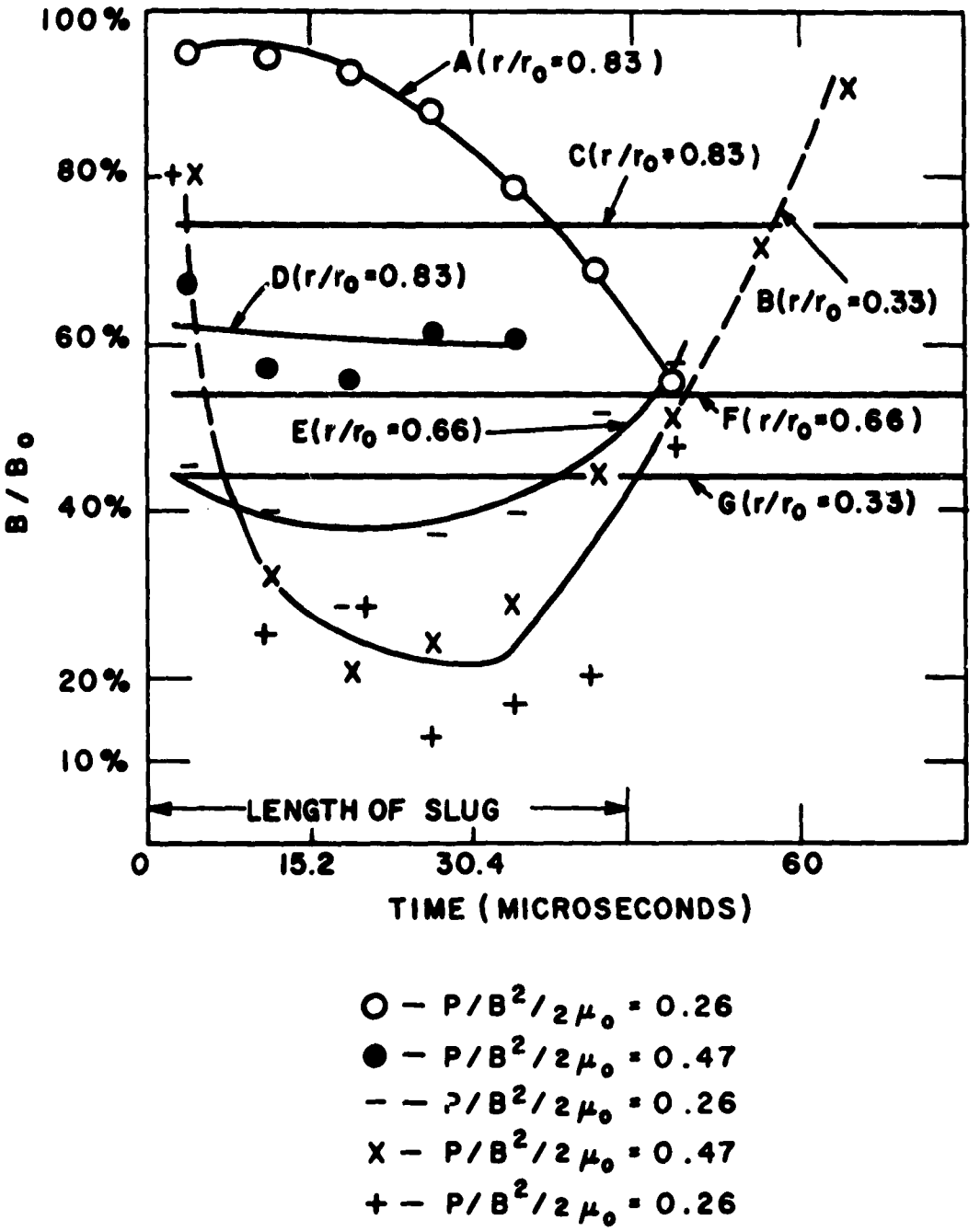

Figure 4. Experimental Measurements of the Local Magnetic Field Inside the Shock Tube (at $r/r_o = 0.83$, $r/r_o = 0.66$ and $r/r_o = 0.33$) for the Moving Plasma Experiments F and G (See Table II) Curves A, E and B Represent the Measurements of B/B_o for Experiment G; and Curves D and B Represent the Measurements of B/B_o for Experiment F. It is to be Noted that at $r/r_o = 0.33$ both Experiment F and G had the Same Value of B/B_o. For Comparison, the Values in Table III under the Heading "Theory" are Reproduced as Lines C, F and G.

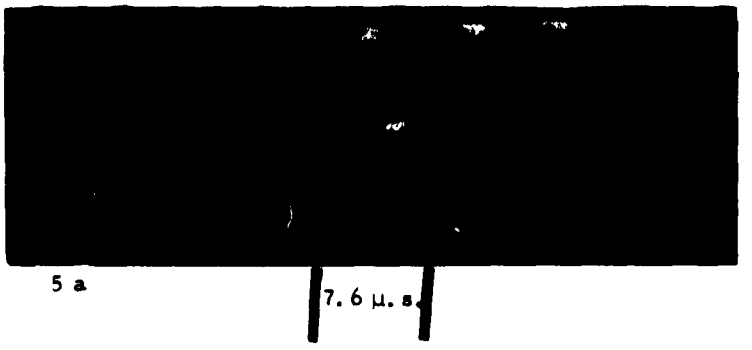

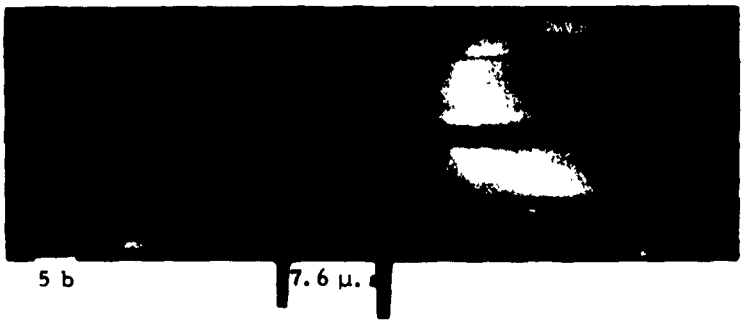

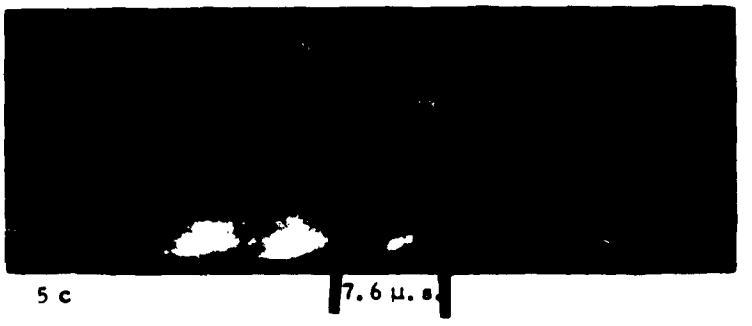

Figure 5. Rotating Mirror Camera Photographs of the Plasma Moving Past the Vertical Slit in the Shock Tube Wall (See Figure 1). Time is from Left to Right and the Scale Marker Beneath Each Photograph Represents 7.6 Microsec. 7.6 Microsec. Equals 1/2 Field Cycle). The Vertical Direction Represents the Slit. The Three Dark Horizontal Lines are Distance Markers Spaced 1.65" Apart, the Central Line Corresponding to the Axis of the Tube. The Thick, Dark Horizontal Line Near the Ends Represents a Magnetic Probe Which Protruded into the Field of Vision of the Slit. Figure 5a is a Photograph of Experiment C (i.e. $P = B^2/2\mu_0$). Figure 5b shows Experiment E (i.e. $P/B^2/2\mu_0 = 0.5$) and Figure 5c Shows Experiment G (i.e. $P/B^2/2\mu_0 = 0.26$).

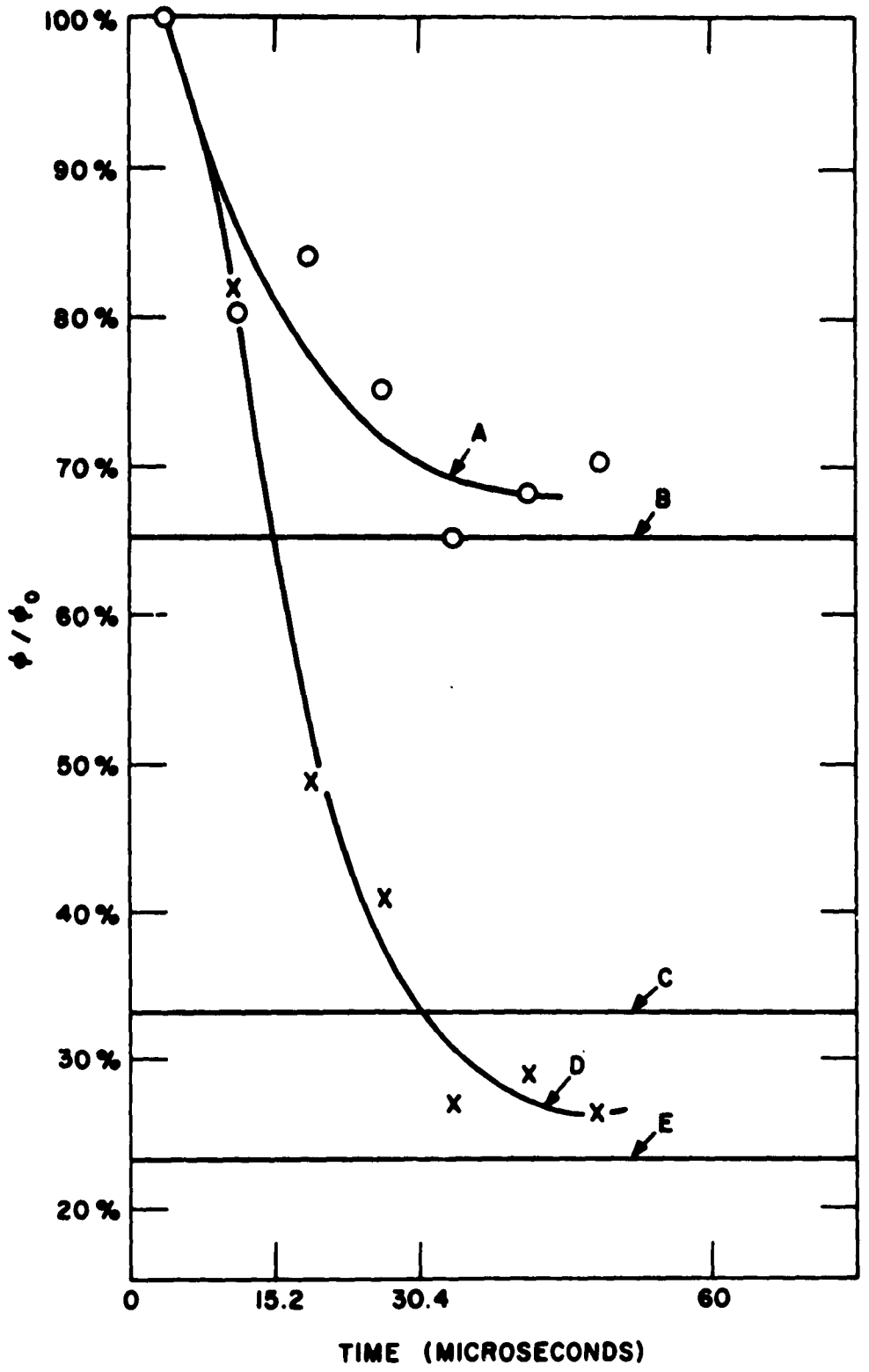

Figure 6. The Peak Values of the Flux Reduction, ϕ/ϕ_0, are Shown Versus Time, for the Ring Discharge Experiments in Argon. Curve A is a Plot of ϕ/ϕ_0 for the 100 Micron Pressure 19 K. V. Capacitor Voltage Experiment While Curve D Represents the 260 Micron, 15 K. V. Experiment. For Comparison with the Moving Plasma Experiments, Line B Represents the Theoretical ϕ/ϕ_0 for a Solid Infinite, 7.5 cm Radius, Cylinder with σ = 3700 mhos/M in a 67 K. c. Field. Line E Represents ϕ/ϕ_0 for $\sigma = \infty$ (i.e. it Shows the Value of the Flux in the Glass Walls of the Shock Tube.

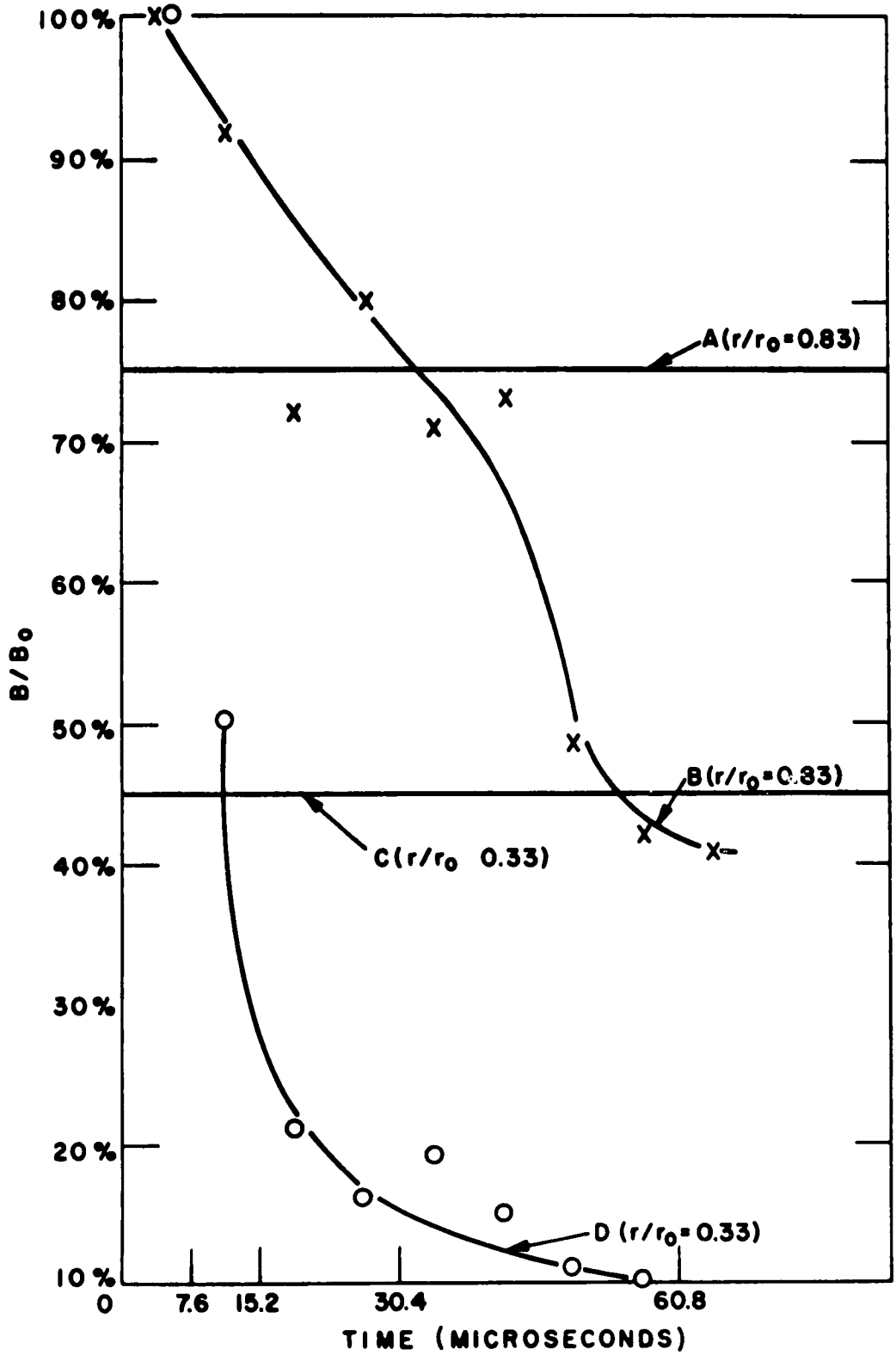

Figure 7. Curves B and D Show the Peak Values of B/B_o (as Measured by Probe No. 7 at $r/r_o = 0.83$ and $r/r_o = 0.33$) Versus Time, for the 260 Microns, 15 K. V. Ring Discharge Experiments. For Comparison with the Moving Plasma Experiments, Line A and C Shows the Values of B/B_o (at $r/r_o = 0.83$ and 0.33) for an Infinite, 7.5 cm Radius, Cylinder of Conductivity 3700 mhos/m. These Values are Taken from the Colum in Table III Under the Heading "Theory". It can be Seen that the Experimental Conductivity is much Higher than 3700 mhos/m.

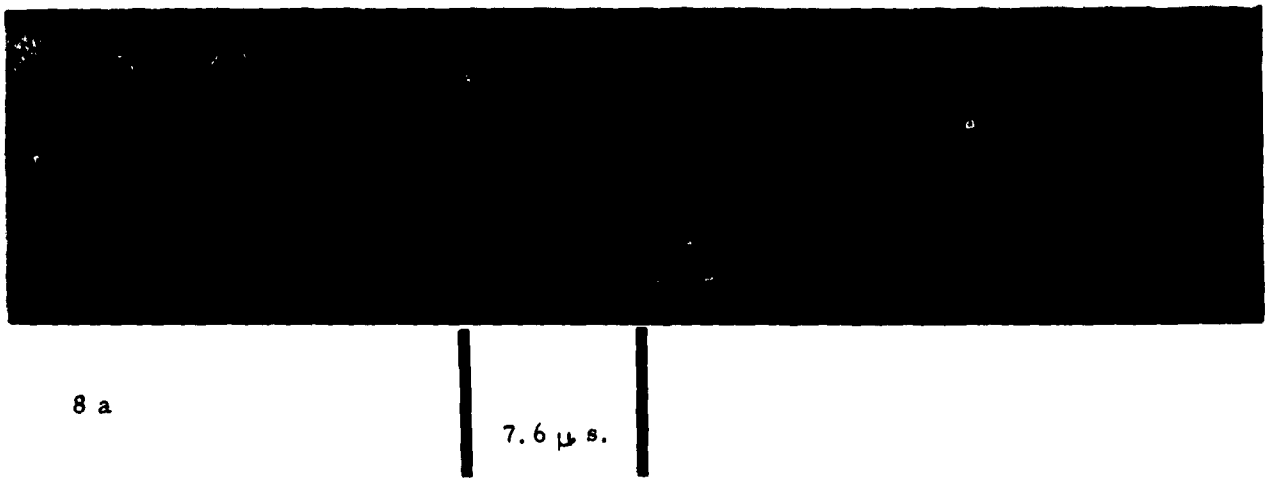

8 a

7.6 μ s.

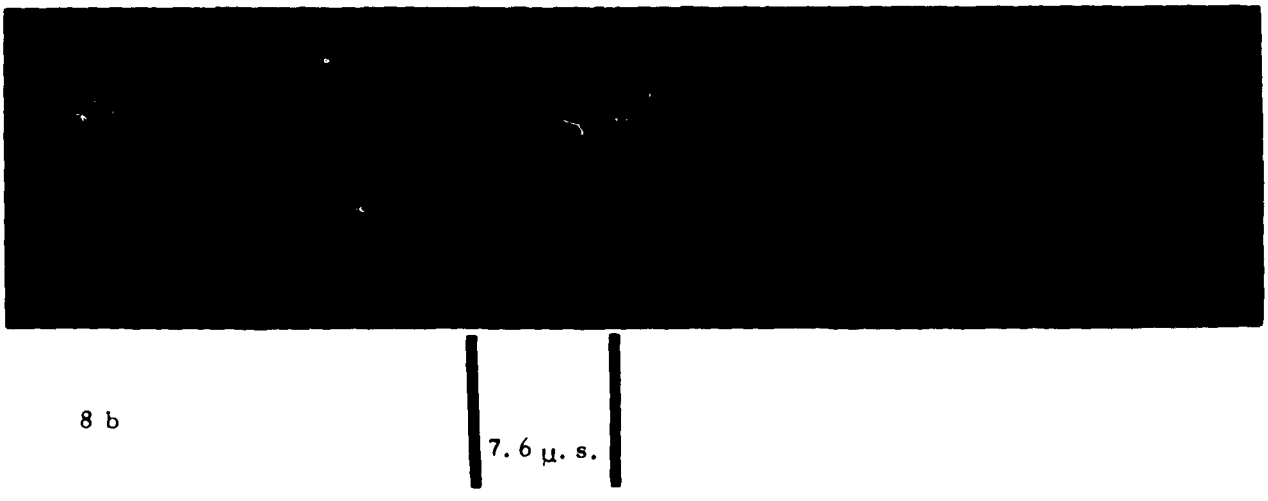

8 b

7.6 μ. s.

Figure 8. Smear Photographs of the Ring Discharge Experiments, Showing the Radial Shock Pattern Observed Versus Time Through a Vertical Slit in the Glass Tube Wall (See Figure 1). Time is From Left to Right and the Scale Marker Beneath Each Photograph Represents 7.6 Microsec. (7.6 Microsec. Equals 1/2 Field Cycle). The Horizontal Lines Have the Same Meaning as in Figure 5. Figure 8a Shows the 260 Micron, 15 K. V. Experiment and Figure 8b Shows the 100 Micron, 19 K. V. Experiment.

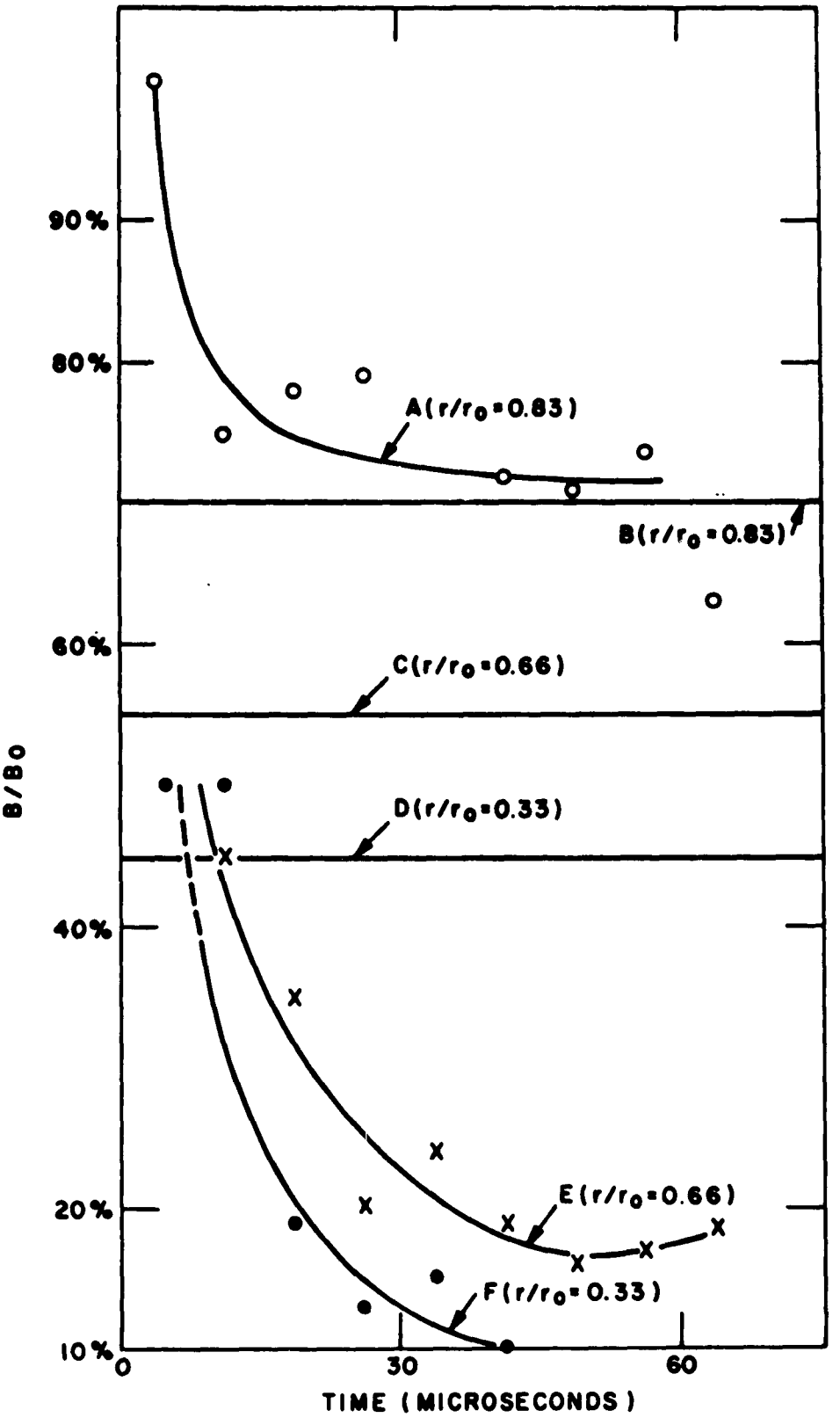

Figure 9. Curve A, E, and F Show the Peak Values of B/B_o (as Measured by Probe No. 7 (See Figure 2) at r/r_o = 0.83, 0.66 and 0.33 Respectively) Versus Time for the 100 Micron, 19 K, V° Ring Discharge Experiment in Argon. For Comparison to the Moving Plasma Experiments the Corresponding Values of B/B_o as Taken From the "Theory" Column in Table III are Shown as Lines B, C and D. It can be Seen That the Experimental Conductivity is much Higher than 3700 mhos/m.

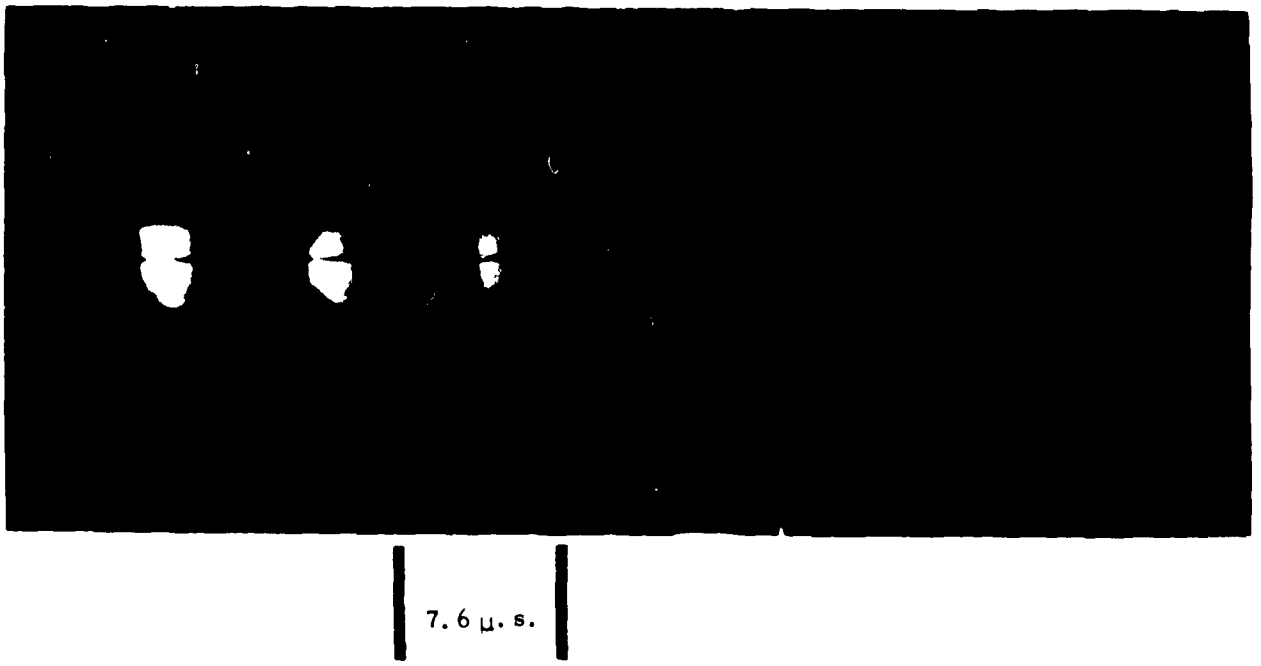

Figure 10. Smear Photograph of Ring Discharge Experiment in Hydrogen at 100 Microns Pressure With a 19 K. V. Capacitor Voltage. This Photograph Shows the Shock Pattern Observed Through a Vertical Slit (See Figure 1) Versus Time. Time is From Left to Right and the Scale Marker Beneath the Photograph Represents 7.6 Microsec. (7.6 μ sec = 1/2 Field Cycle). The Three Thin Horizontal Lines are Distance Markers, and the Two Thick Horizontal Lines are Photographs of Magnetic Probes Which Protrude into the Field of Vision of the Slit.

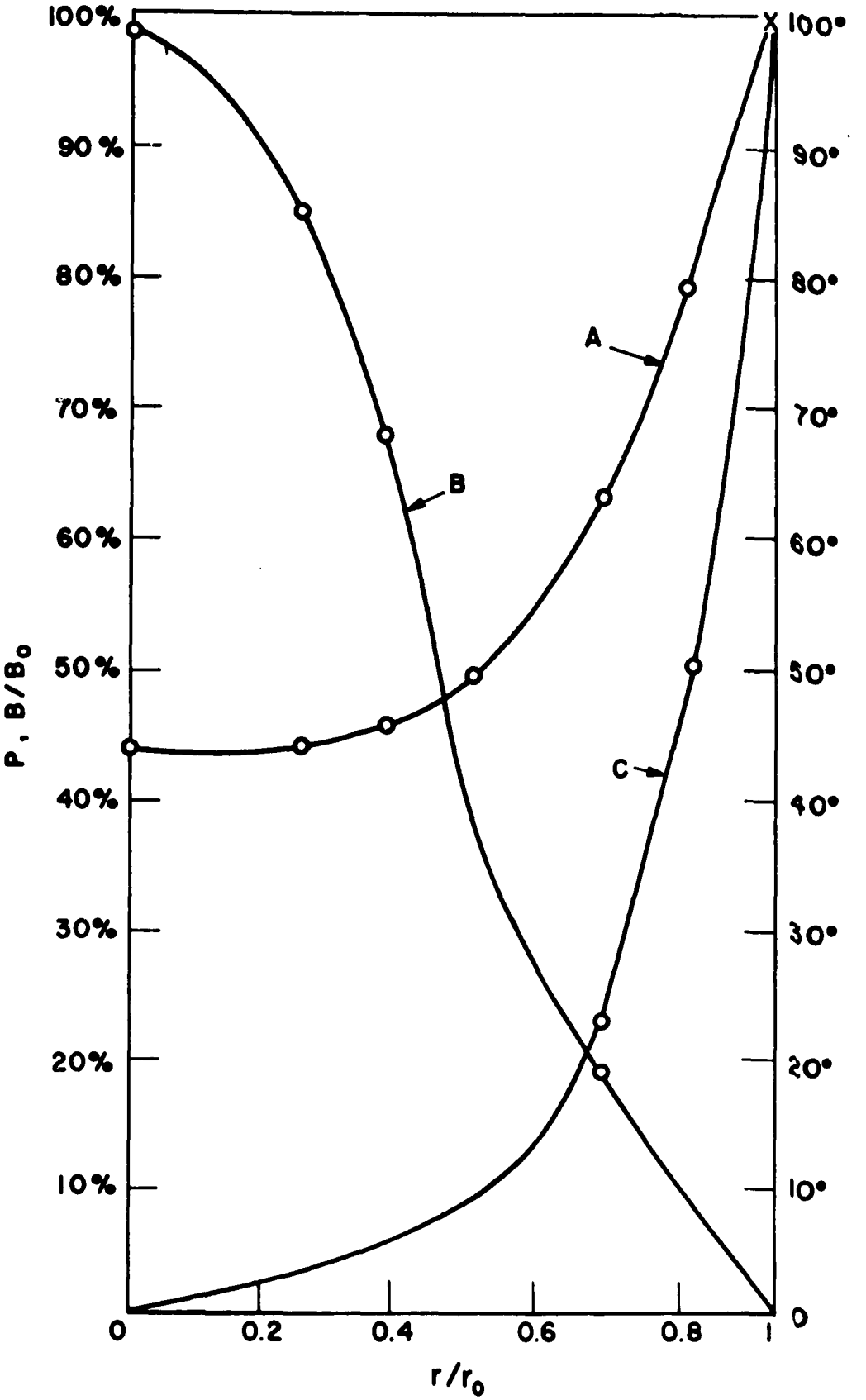

Figure 11. Curve A Represents a Theoretical Plot of B/B_0 Versus r/r_0 for an Infinite, Solid, Cylinder, of Radius $r_0 = 7.5$ cm with $\sigma = 3700$ mhos/m, in a Coaxial 67 K. C. Magnetic Field. Curve B Represents the Phase Shift $(\theta_0[p^{1/2}r] - \theta_0[P^{1/2}r_0]$ for this Cylinder and Curve C is a Plot of $P = P_r/P_{r_0}$ Versus r/r_0 for this Cylinder.

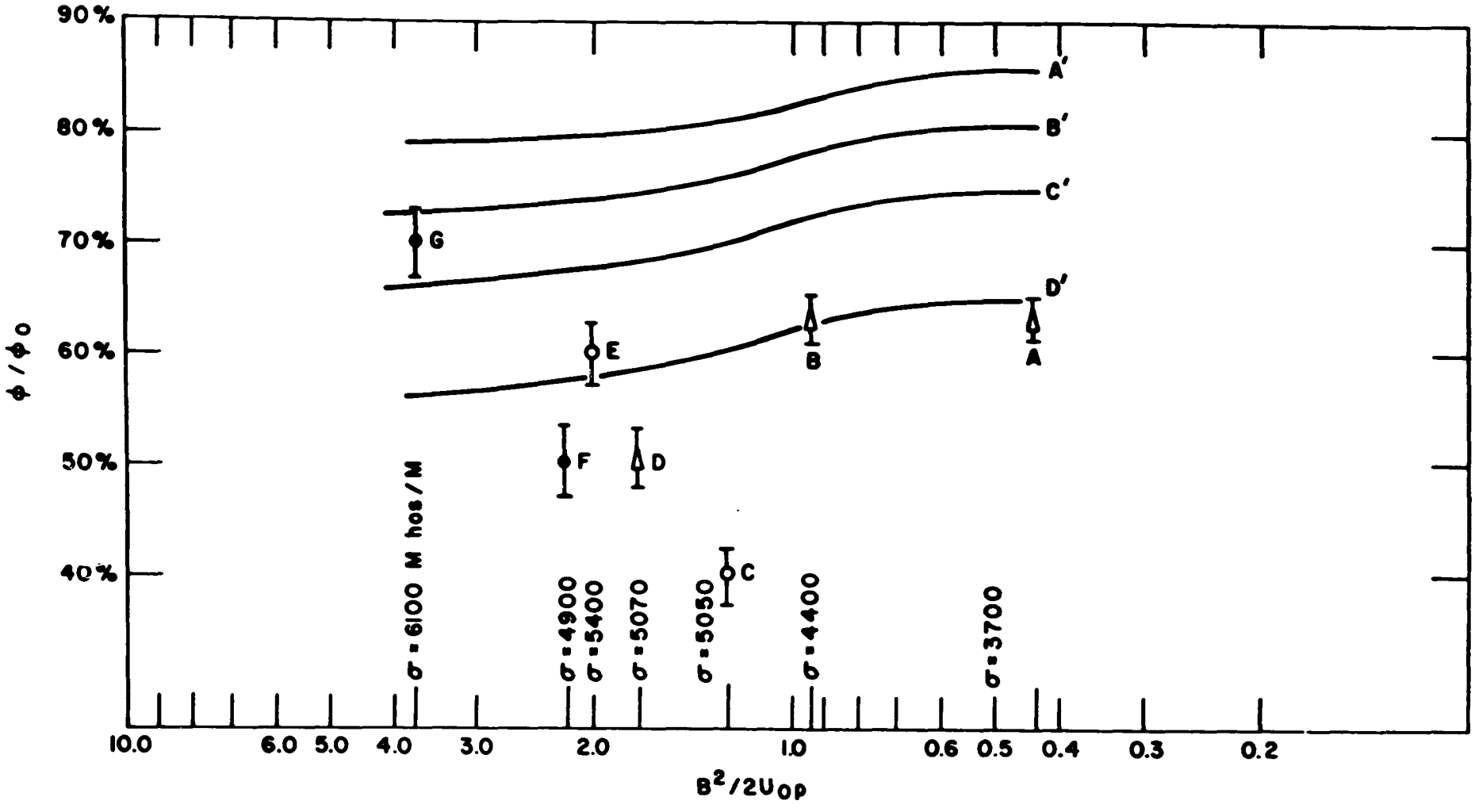

Figure 12. Curves A', B', C' and D' Show the Theoretical Values of ϕ/ϕ_0 Versus $B^2/2\mu_0 P$ Computed by Using the Single Conductor Eddy Current Theory Developed in Part V Section b and c. The Values of the Conductivity Used in Making the Computations are Shown on the Horizontal Axis. For Reference, the Experimental Values of ϕ/ϕ_0 (as Plotted in Figure 3) are Also Reproduced.